Cooperative B-H bond activation: Dual sites borane activation by redox active κ²-*N,S*-chelated complexes

Mohammad Zafar,[†a] Asif Ahmad,[†a] Suvam Saha,[a] Rongala Ramalakshmi,[a] Thierry Roisnel[b] and Sundargopal Ghosh*[a]

[a]*Department of Chemistry, Indian Institute of Technology Madras, Chennai 600036, India. Tel: +91 44- 22574230; Fax: +91 44-22574202; E-mail: sghosh@iitm.ac.in*

[b]*Universitéde Rennes, CNRS, Institut des Sciences Chimiques de Rennes, UMR 6226, F-35000 Rennes, France*

† These authors contributed equally to this work

Table of Contents

III References

I Experimental Details

General procedure and instrumentations

All manipulations were conducted by using standard Schlenk line and glove box techniques under an atmosphere of dry argon. Solvents such as toluene, hexane and THF were distilled through Na/benzo-phenoneketyl and dichloromethane was dried over calcium hydride prior to use under argon. Chloroform-d was degassed by three freeze-thaw cycles, dried over calcium hydride for 12 h, and stored over 4 Å molecular sieves in a Young's ampoule under argon. Compounds [(κ²-*N,S*-($C_7H_4NS_2$)R_3PRu{κ³-H,S,S'-H_2B-($C_7H_4NS_2$)$_2$}] (R = Cy, Ph),[1] mesityl borane,[2] were synthesized according to the literature procedures.[1-2] and other chemicals such as BH_3.SMe_2, BH_3.THF, HBPin, catecholborane, 9-Borabicyclo[3.3.1]nonane solution (9-BBN) were obtained commercially (Sigma Aldrich) and used as received. The external reference for the ^{11}B NMR spectroscopy, [Bu_4N][(B_3H_8)] was synthesized according to the literature method.[3] The ^{1}H, ^{11}B{^{1}H}, ^{13}C{^{1}H}, and ^{31}P{^{1}H} NMR spectra were recorded on Bruker 400 and 500 MHz instruments. The residual solvent protons were used as reference (δ, ppm, benzene-d_6, 7.16, $CDCl_3$, 7.26, Toluene-d_8, 7.09 ppm), while a sealed tube containing [Bu_4N][(B_3H_8)] in benzene-d_6 (δ_B, ppm, -30.07) was used as an external reference for ^{11}B{^{1}H} NMR spectra. ^{1}H decoupled ^{11}B{^{1}H} spectra of all compounds were processed with a backward linear prediction algorithm to remove the broad ^{11}B{^{1}H} background signal of the NMR tube.[4] The preparative TLC was performed with Merck 105554 TLC silica gel 60 F254 and thickness of layer 250 µm on aluminum sheets with 20x20 cm size. Mass spectra were carried out using Qtof Micro YA263 HRMS instrument and Bruker MicroTOF-II mass spectrometer in ESI ionization mode. UV-vis absorption spectra were gained from Jasco V-650 spectrometer. Infrared spectra were obtained on a Jasco FT/IR–1400 spectrometer.

I.1 Synthesis and Characterizations

Syntheses of *mer*-**2a** and **2b**: In a flame-dried NMR tube *trans-mer*-[(κ²-*N,S*-($C_7H_4NS_2$)Cy_3PRu{κ³-H,S,S'-H_2B-($C_7H_4NS_2$)$_2$}], **1a** (30 mg, 34 µmol) in 1.5 mL choloroform-*d* solvent and the solution kept in open air at room temperature. After 2 days standing at room temperature dark green solution was formed. The volatile components were removed under vacuum and remaining residue was extracted into CH_2Cl_2/hexane and passed through celite. After removal of the solvent, the residue was subjected to chromatographic work-up by using TLC plates. Elution with a *n*-hexane/CH_2Cl_2 (70:30 v/v) yielded green solid *mer*-**2a** (18 mg, 62%).

Under similar reactions conditions, reaction of *trans-mer*-[(κ²-*N,S*-($C_7H_4NS_2$)-PPh_3PRu{κ³-H,S,S'-H_2B-($C_7H_4NS_2$)$_2$}], **1b** (30 mg, 33 µmol) yielded green solid *mer*-**2b** (16mg, 55%).

mer-**2a**: MS (ESI⁺): *m/z* calculated for [$C_{39}H_{45}N_3PRuS_6$ + H]⁺: 881.0797, found 881.0789.

mer-**2b**: MS (ESI⁺): *m/z* calculated for [$C_{39}H_{27}N_3PRuS_5$ + H]⁺: 862.9388, found 862.9324.

Syntheses of *fac*-**3a** and **3b**: In a flame-dried Schlenk tube, *mer*-[(κ²-*N,S*-($C_7H_4NS_2$)$_2Cy_3$PRu{κ¹-*S*-($C_7H_4NS_2$)}], **2a** (30 mg, 34 µmol) in 5 mL dry toluene was treated with excess BH_3.THF at room temperature. The reaction mixture was allowed to stir at room temprerature for 1h. The volatile components were removed under vacuum and the remaining residue was extracted into CH_2Cl_2/hexane and passed through Celite. After removal of the solvent, the residue was subjected to chromatographic work-up by using TLC plates. Elution with a *n*-hexane/CH_2Cl_2 (80:20 v/v) mixture yielded yellow solid *fac*-**3a** (10 mg, 38%).

Under similar reactions conditions, reaction of *mer*-[(κ²-*N,S*-($C_7H_4NS_2$)$_2$-PPh_3PRu{κ¹-*S*-($C_7H_4NS_2$)}], **2b** (30 mg, 34 µmol) with excess BH_3.THF yielded yellow solid *fac*-**3b** (11 mg, 42%).

fac-**3a**: MS (ESI⁺): *m/z* calculated for [$C_{32}H_{45}B_2N_2PRuS_5$]⁺: 772.1167, found 772.1165; ^{11}B{^{1}H} NMR (160 MHz, $CDCl_3$, 22 °C): *δ* -11.5 ppm (br, B); ^{1}H NMR (500 MHz, $CDCl_3$, 22 °C): *δ* 7.87 (d, J = 8.2 Hz, 2H, $Ar_{(mbz)}$), 7.44 (t, J = 8.6 Hz, 4H, $Ar_{(mbz)}$), 7.37 (dd, J = 10.4, 8.0 Hz, 6H, Ar), 7.33 (d, J = 6.8 Hz, 2H, $Ar_{(mbz)}$), 7.29 (t, J = 8.1 Hz, 8H, Ar), 7.26 (d, J = 2.7 Hz, 1H, Ar), 2.97 (d, 2H, B-H_t), 1.85-1.64 (m, 33H), -14.34 ppm (br, 2H, Ru-H-B); ^{13}C{^{1}H} NMR (125 MHz, $CDCl_3$, 22 °C): *δ* 26.7- 36.7 (Cy), 116.0-133.6 (Ph), 144.6 (C-N), 193.7 (C=S) ppm; ^{31}P{^{1}H} NMR (202 MHz, $CDCl_3$, 22 °C): *δ* 71.0 ppm; IR (CH_2Cl_2): ṽ = 2443 (B-H_t), 1961 cm^{-1} (B-H_b).

fac-**3b**: MS (ESI⁺): *m/z* calculated for [$C_{32}H_{27}B_2N_2PRuS_5$ + Na]⁺: 776.9660, found 776.9636; ^{11}B{^{1}H} NMR (160 MHz, $CDCl_3$, 22 °C): *δ* -10.1 ppm (br, B); ^{1}H NMR (500 MHz, $CDCl_3$, 22 °C):, *δ* 7.87 (d, J = 8.3 Hz, 1H, $Ar_{(mbz)}$), 7.43 (t, J = 7.4 Hz, 2H, $Ar_{(mbz)}$), 7.26 (d, J = 2.9 Hz, 3H, $Ar_{(mbz)}$), 3.01 (d, 2H, B-H_t), -13.24 ppm (br, 1H, Ru-H-B); ^{13}C{^{1}H} NMR (125 MHz, $CDCl_3$, 22 °C): *δ* 116.0-137.4 (Ph) 144.4 (C-N) 194.0 (C=S) ppm; ^{31}P{^{1}H} NMR (202 MHz, $CDCl_3$, 22 °C): *δ* 60.9 ppm; IR (CH_2Cl_2): ṽ = 2403 (B-H_t), 1991 cm^{-1} (B-H_b).

Syntheses of *fac*-**3c**: In a flame-dried Schlenk tube, cis-*fac*-[(κ²-*N,S*-(C_5H_4NS)Ph_3PRu{κ³-H,S,S'-H_2B-(C_5H_4NS)$_2$}], *cis-fac*-**1a** (50 mg, 70 µmol) in 10 mL dry toluene was treated with excess BH_3.THF at room temperature. The reaction mixture was allowed to stir at room temprerature for 2h. The volatile components were removed under vacuum and the remaining residue was extracted into CH_2Cl_2/hexane and passed through Celite. After removal of the solvent, the residue was subjected to chromatographic work-up by using TLC plates. Elution with a *n*-hexane/CH_2Cl_2 (75:25 v/v) mixture yielded yellow solid *fac*-**3c** (18 mg, 39%).

fac-**3c**: MS (ESI$^+$): *m/z* calculated for $[C_{28}H_{27}B_2N_2PRuS_3]^+$: 642.0321, found 642.0321; $^{11}B\{^1H\}$ NMR (160 MHz, $CDCl_3$, 22 °C): δ -3.8 ppm (br, B); ^1H NMR (400 MHz, $CDCl_3$, 22 °C): δ 8.03 (d, J = 6.3 Hz, 2H $Ar_{(mp)}$), 7.46 (d, J = 8.6 Hz, 2H $Ar_{(mp)}$), 7.42 – 7.20 (m, 15H Ph), 7.09 (s, 2H, $Ar_{(mp)}$), 6.67 (s, 2H $Ar_{(mp)}$), 2.80 (d, $J_{H\text{-}H}$ = 13.1 Hz, 2H, B-H_t), -12.27 ppm (m, 2H, Ru-H-B); $^{13}C\{^1H\}$ NMR (125 MHz, $CDCl_3$, 22 °C): δ 114.4-128.0 ($Ar_{(mp)}$), 129.3-133.4 (Ph), 137.6-138.1 (C-S), 145.1 (C-N), 179.7 (C=S) ppm; $^{31}P\{^1H\}$ NMR (202 MHz, $CDCl_3$, 22 °C): δ 60.8 ppm; IR (CH_2Cl_2): $\tilde{\nu}$ = 2443 (B-H_t), 1961 cm^{-1} (B-H_b).

Syntheses of *trans*-**4** and *cis*-**4**: In the glovebox, mesitylborane (11 mg, 87 µmol) was added to a solution of [(κ^2-*N,S*-$(C_7H_4NS_2)_2PPh_3Ru\{\kappa^1$-*S*-$(C_7H_4NS_2)\}]$, **2b** (30 mg, 34 µmol) in dry toluene (5mL). The reaction mixture was allowed to stir at 90 °C temperature for 12 h. The volatile components were removed under vacuum and red colour was washed with 4 × 5 mL of hexane to give inseparable yellow solid mixture of *trans* and *cis* isomers of compound **4** (16 mg, 45%). We report the combined spectroscopic data for *trans*-**4** and *cis*-**4**.

Combined spectroscopic data for *trans*-**4** and *cis*-**4**: MS (ESI$^+$): *m/z* calculated for $[C_{32}H_{34}B_2N_2RuS_4]^+$: 698.0849, found 698.0799; $^{11}B\{^1H\}$ NMR (160 MHz, Toluene-d_8, 22 °C): δ 39.4 ppm (br, B) for *trans*-**4** and 31.2 ppm (br, B) for *cis*-**4**; $^1H\{^{11}B\}$ NMR (500 MHz, Benzene-d_6, 22 °C): δ –11.42 (br, 4H, Ru-H-B) for *trans*-**4** and –10.41 (br, 2H, Ru-H-B), –10.01 (br, 2H, Ru-H-B) for *cis*-**4,** 2.47 (s, 6H, $CH_{3(Mes)}$), 2.31 (s, 3H, $CH_{3(Mes)}$) mesityl proton for *trans*-**4** and 2.35 (s, 3H, $CH_{3(Mes)}$), 2.31 (s, 3H, $CH_{3(Mes)}$), 2.27 (s, 3H, $CH_{3(Mes)}$) mesityl proton for *cis*-**4**, [7.69-6.53 ppm (all the mesityl and mercaptobenzothaizolyl aromatic proton) for *trans*-**4** and *cis*-**4**]; $^{13}C\{^1H\}$ NMR (125 MHz, Toluene-d_8, 22 °C): δ 22.7 (CH_3^{ortho}, Mes), 20.4 (CH_3^{para}, Mes) for *trans*-**4** and 22.5 (CH_3^{ortho}, Mes), 22.3 (CH_3^{ortho}, Mes). 20.2 (CH_3^{para}, Mes) for *cis*-**4**, [140.8-114.7 ppm (all the mesityl and mercaptobenzothaizolyl aromatic carbon for *trans*-**4** and *cis*-**4**] 143.4-144.3 (C-N), 193.6-195.8 (C=S) *trans*-**4** and *cis*-**4**; IR (CH_2Cl_2): $\tilde{\nu}$ = 1945 cm^{-1} (B-H_b) for *trans*-**4** and 1941 cm^{-1} (B-H_b) for *cis*-**4**.

I.2 Spectroscopic Details

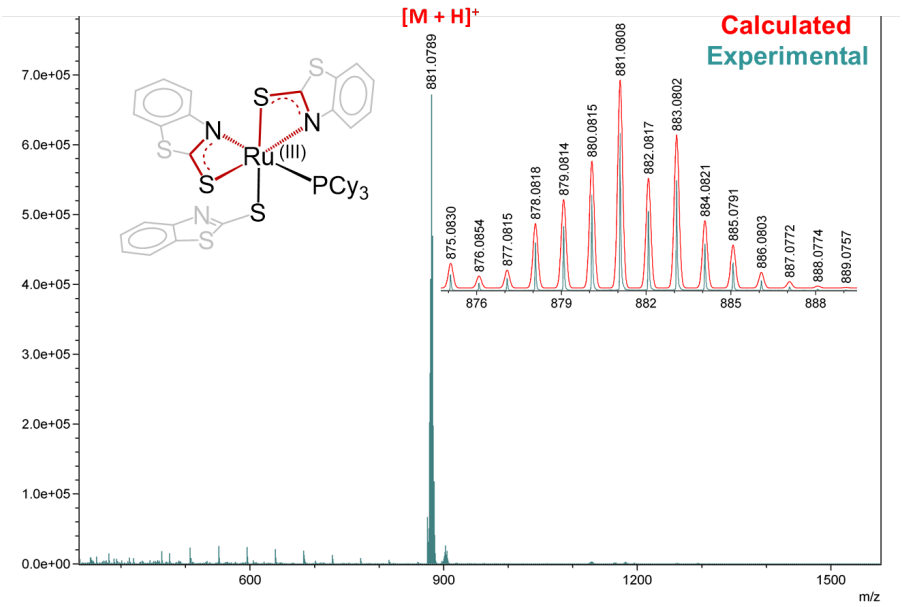

Figure S1. Calculated (red) and experimental (green) mass spectral isotopic distribution for the fragment of *mer*-**2a**.

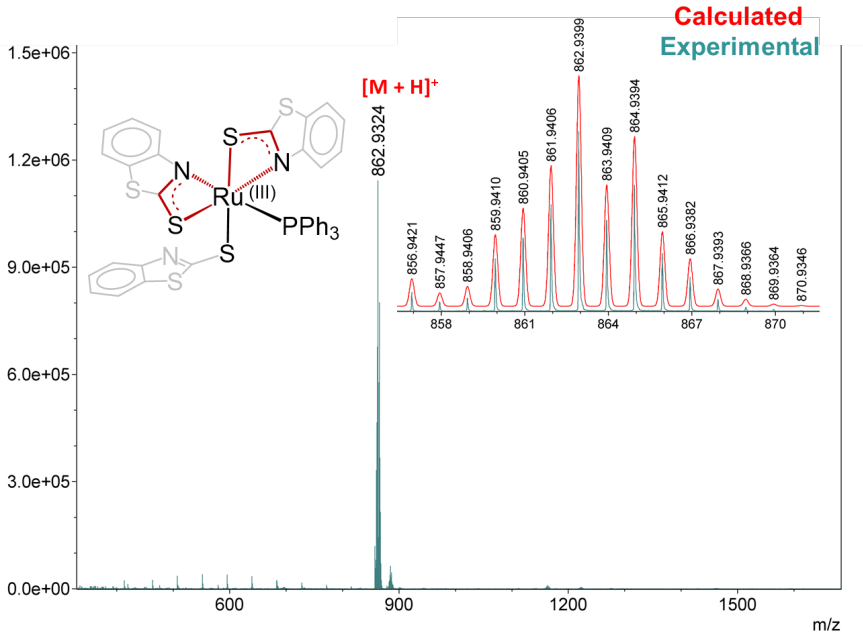

Figure S2. Calculated (red) and experimental (green) mass spectral isotopic distribution for the fragment of *mer*-**2b**.

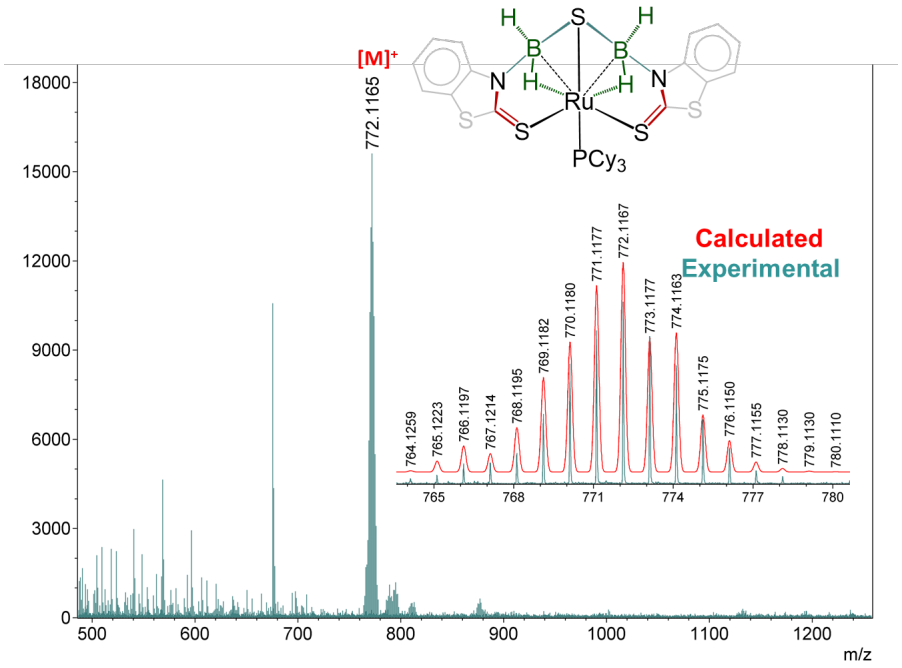

Figure S3. Calculated (red) and experimental (green) mass spectral isotopic distribution for the fragment of *fac*-**3a**.

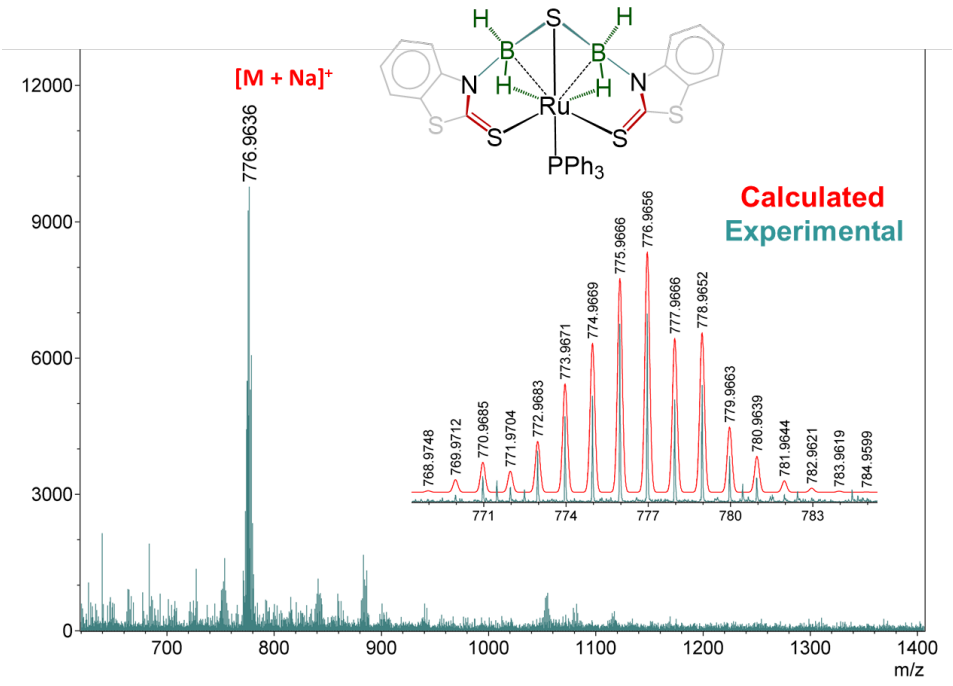

Figure S4. Calculated (red) and experimental (green) mass spectral isotopic distribution for the fragment of *fac*-**3b**.

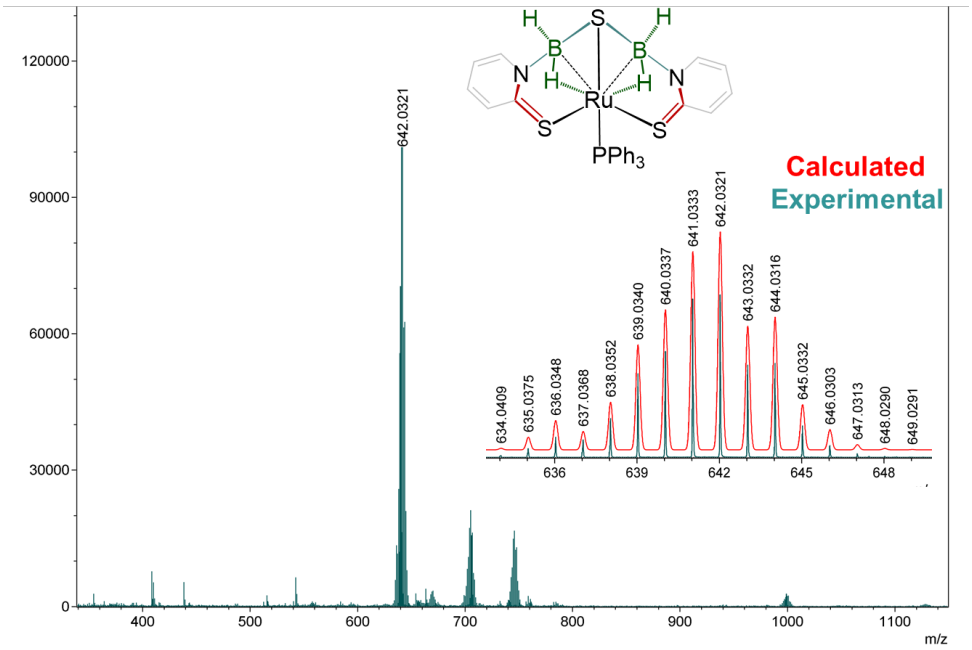

Figure S5. Calculated (red) and experimental (green) mass spectral isotopic distribution for the fragment of *fac*-**3c**.

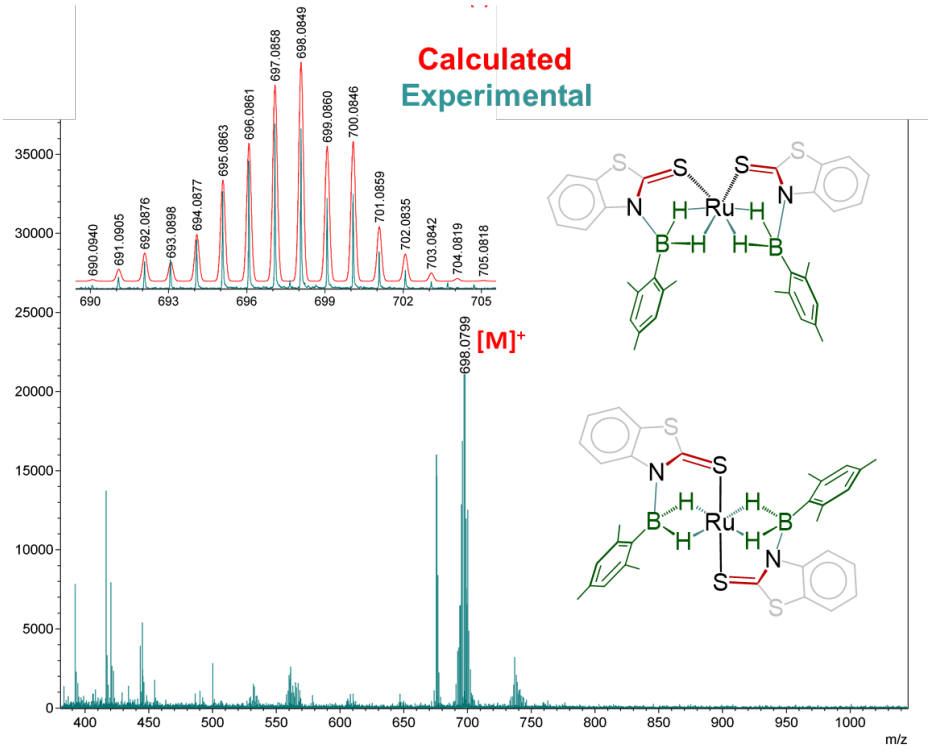

Figure S6. Combined calculated (red) and experimental (green) mass spectral isotopic distribution for the fragment of *trans*-**4** and *cis*-**4**.

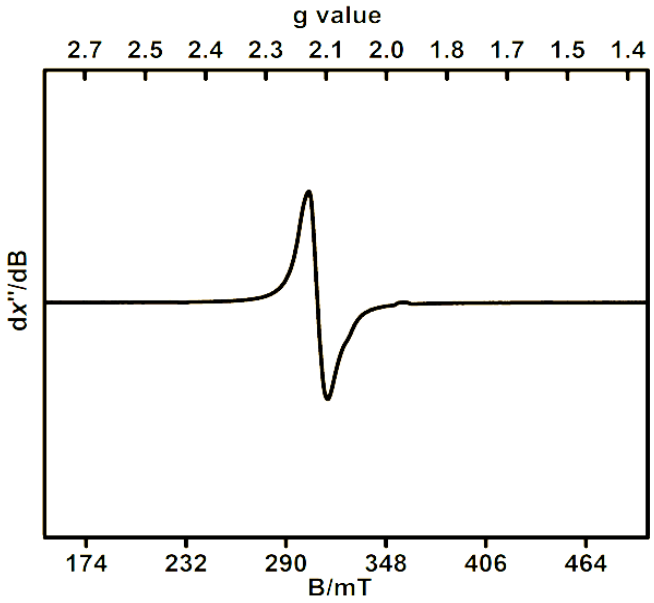

Figure S7. EPR spectrum of *mer*-**2b**.

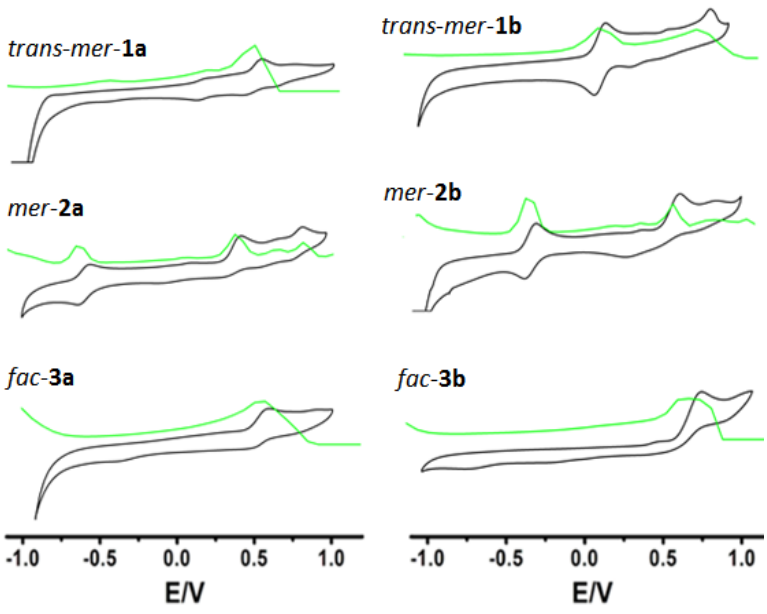

Figure S8. Cyclic voltammetry of *trans-mer*-**1a**, *mer*-**2a** and *fac*-**3a** (left), *trans-mer*-**1b**, *mer*-**2b** and *fac*-**3b** (right) collected at 100 mv/s as well as their differential pulse voltammetry (green). All CV data were collected in CH_3CN with 0.1 M $(nBu_4N)PF_6$ using a glassy carbon working electrode, Pt wire counter electrode, and Ag/AgCl-reference electrode.

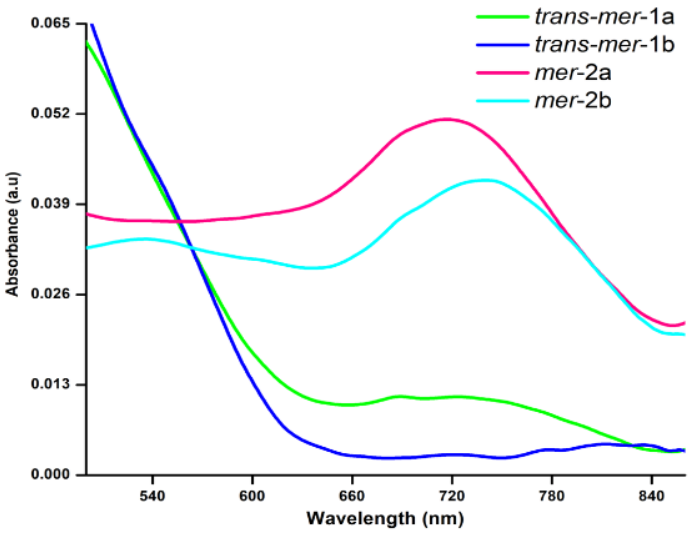

Figure S9. Comparison of UV-Vis/NIR spectra of *mer*-**2a-b** and *trans-mer*-**1a-b** in dichloromethane.

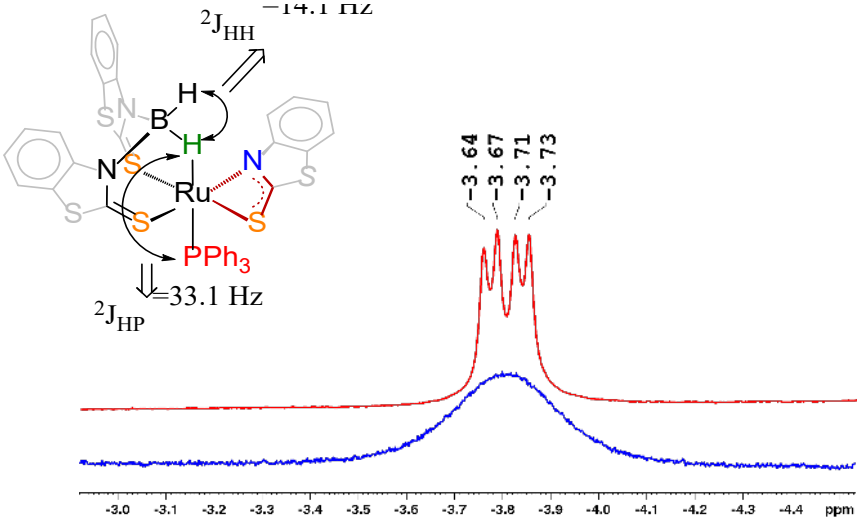

Figure S10. Combined ^{1}H NMR and $^{1}H\{^{11}B\}$ NMR spectra of complex *trans-mer*-**1b** in $CDCl_3$ (500 MHz).

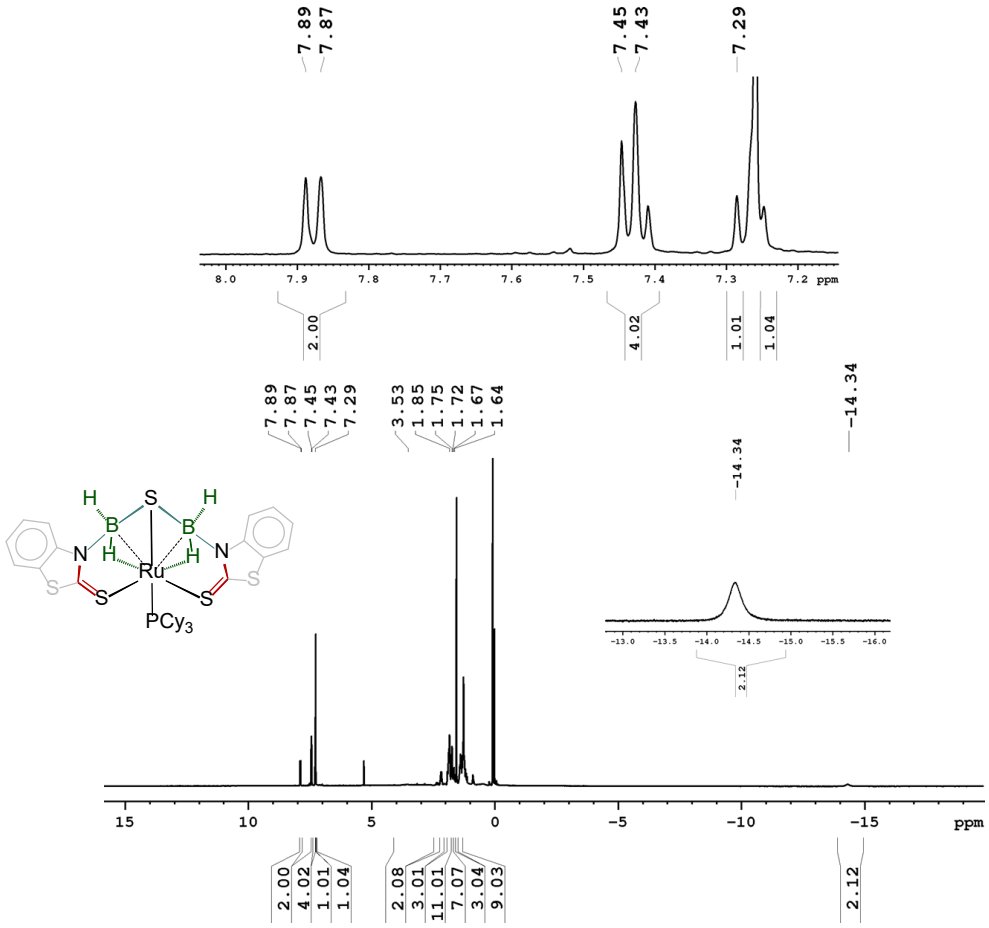

Figure S11. ^{1}H NMR spectrum of the complex *fac*-**3a** in $CDCl_3$ (500 MHz).

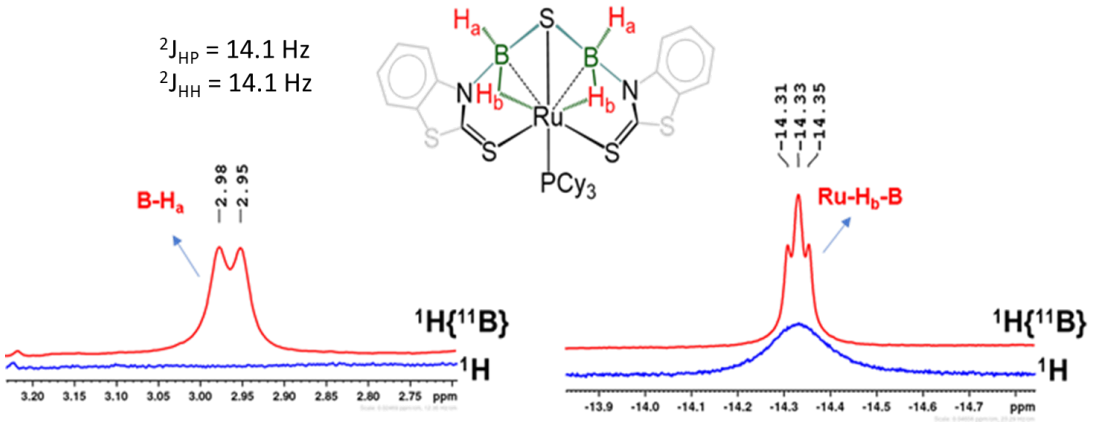

Figure S12. Combined ^{1}H NMR and ^{1}H{^{11}B} NMR spectra of complex *fac*-**3a** in $CDCl_3$ (500 MHz).

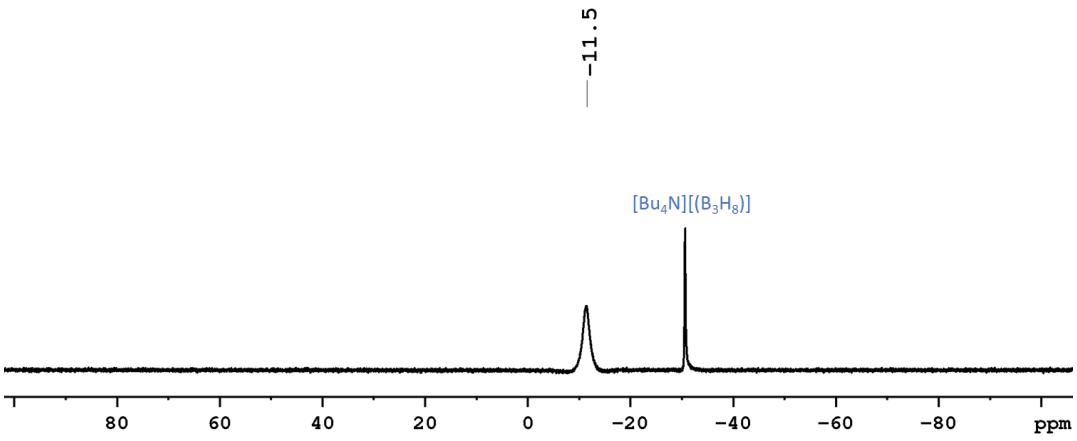

Figure S13. $^{11}B\{^{1}H\}$ NMR spectrum of the complex *fac*-**3a** in $CDCl_3$ (160 MHz).

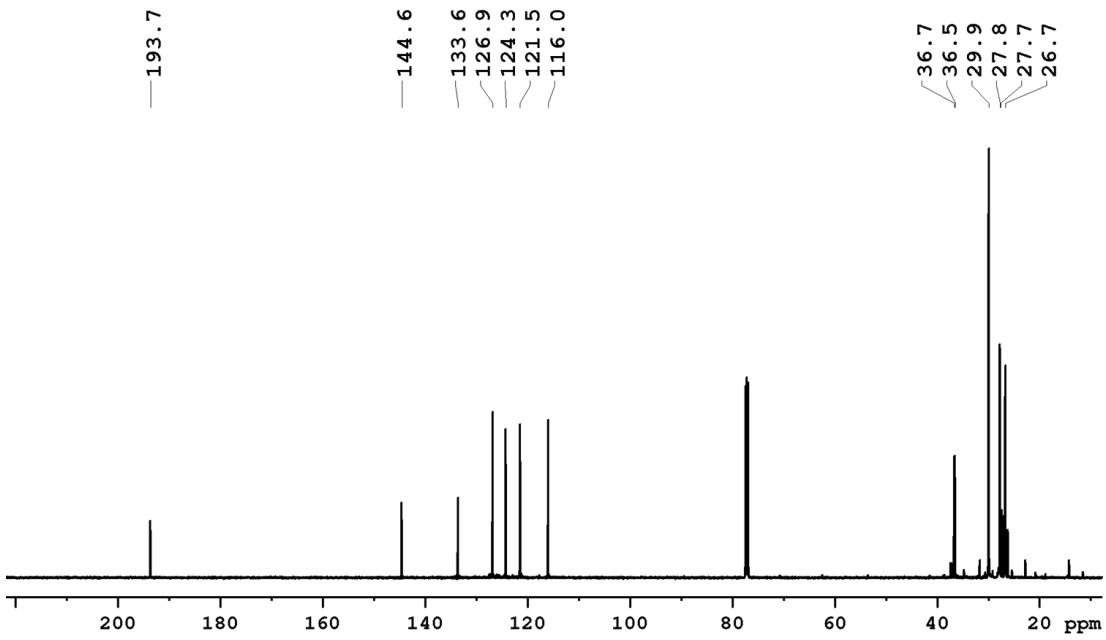

Figure S14. $^{13}C\{^{1}H\}$ NMR spectrum of the complex *fac*-**3a** in $CDCl_3$ (125 MHz). (•=.solvent and grease impurities).

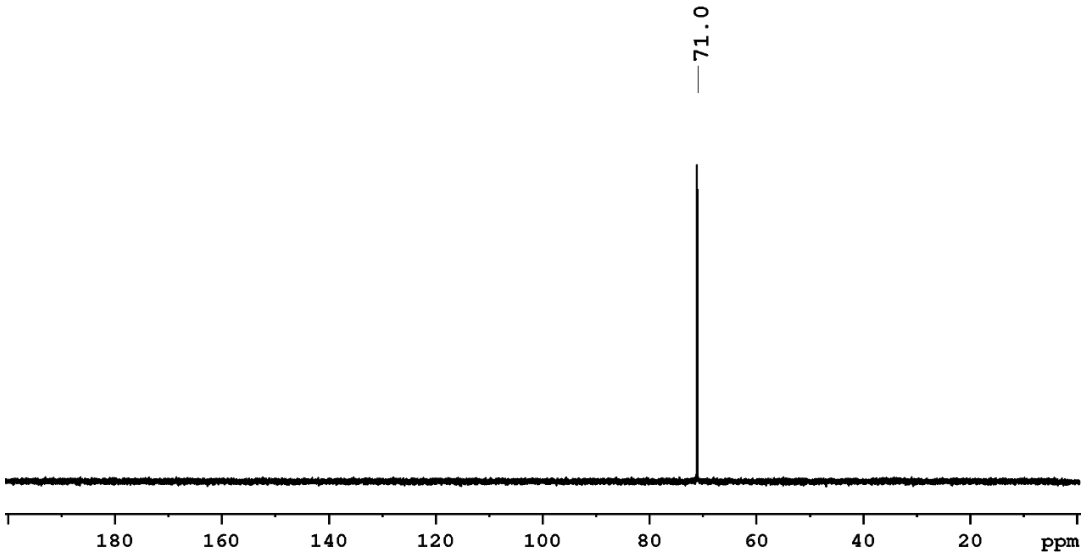

Figure S15. $^{31}P\{^{1}H\}$ NMR spectrum of the complex *fac*-**3a** in $CDCl_3$ (202 MHz).

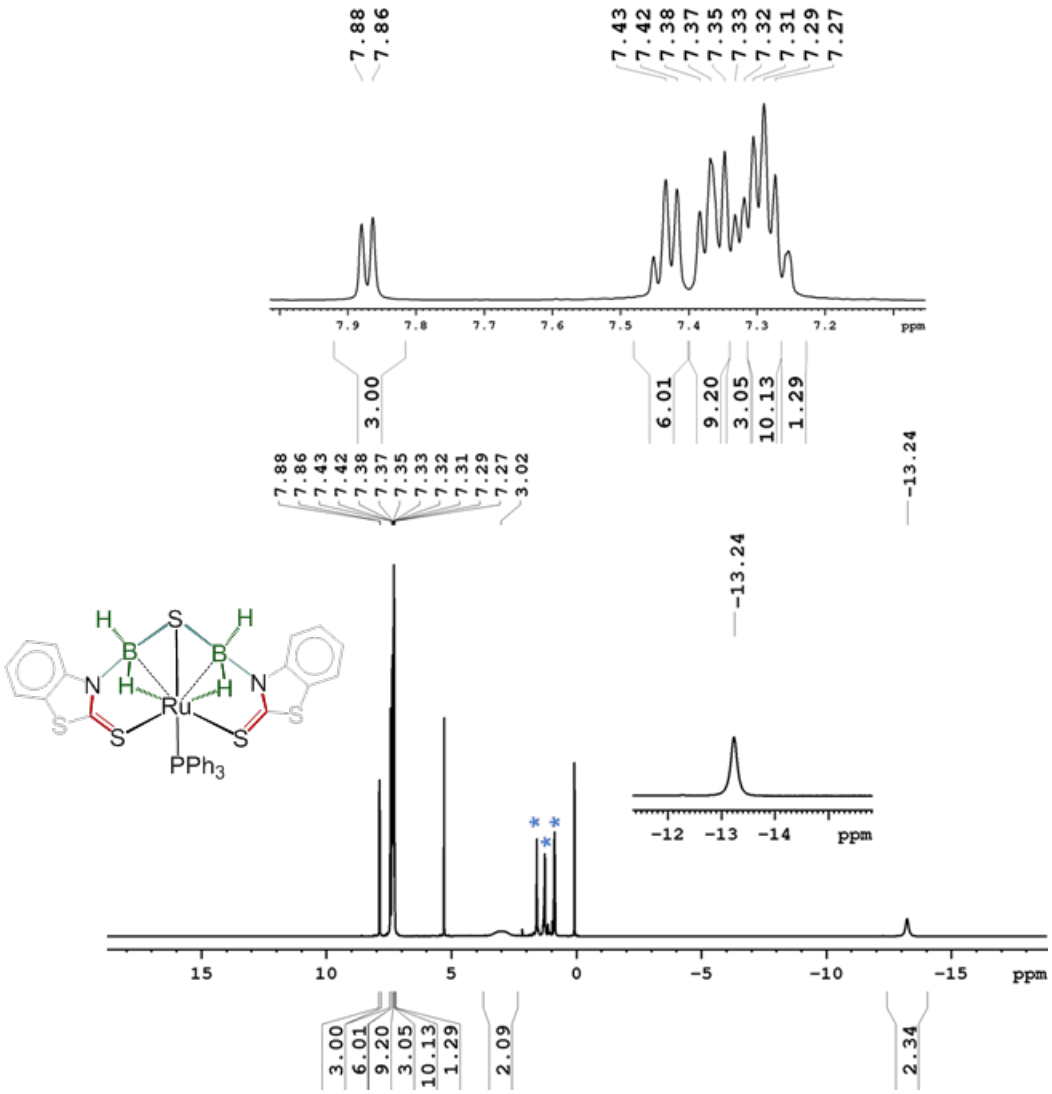

Figure S16. ^{1}H NMR spectrum of the complex *fac*-**3b** in $CDCl_3$ (500 MHz) (•=.solvent and grease impurities).

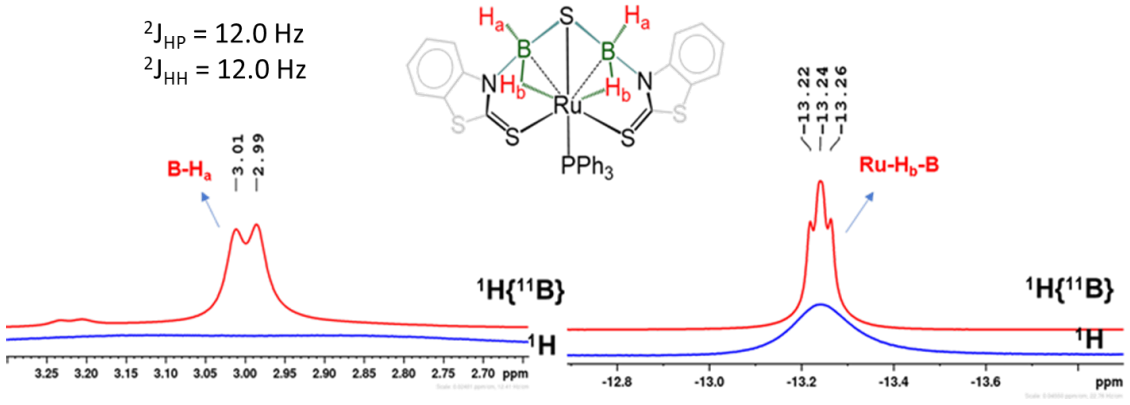

Figure S17. Combined ^{1}H NMR and ^{1}H{^{11}B} NMR spectra of complex *fac*-**3b** in $CDCl_3$ (500 MHz).

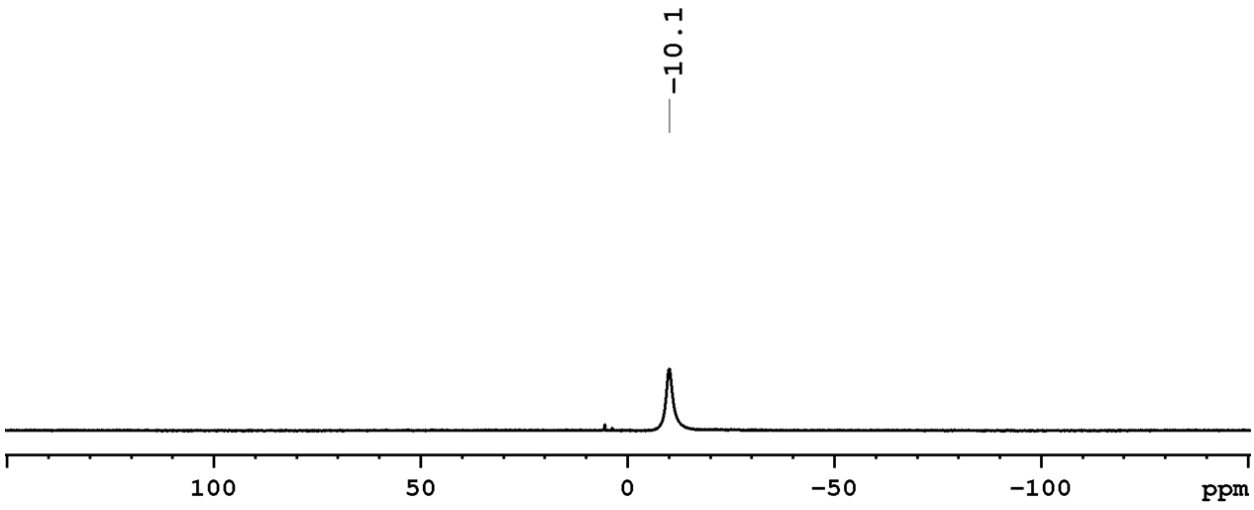

Figure S18. ^{11}B{^{1}H} NMR spectrum of the complex *fac*-**3b** in $CDCl_3$ (160 MHz).

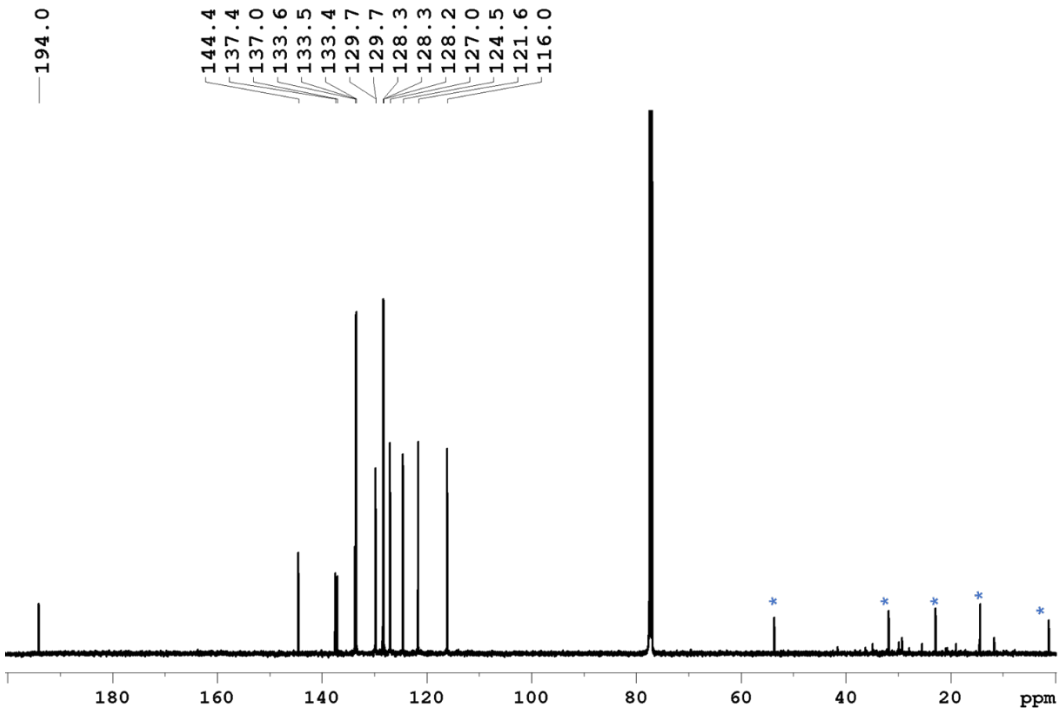

Figure S19. $^{13}C\{^{1}H\}$ NMR spectrum of the complex *fac*-**3b** in $CDCl_3$ (125 MHz). (•=.solvent and grease impurities).

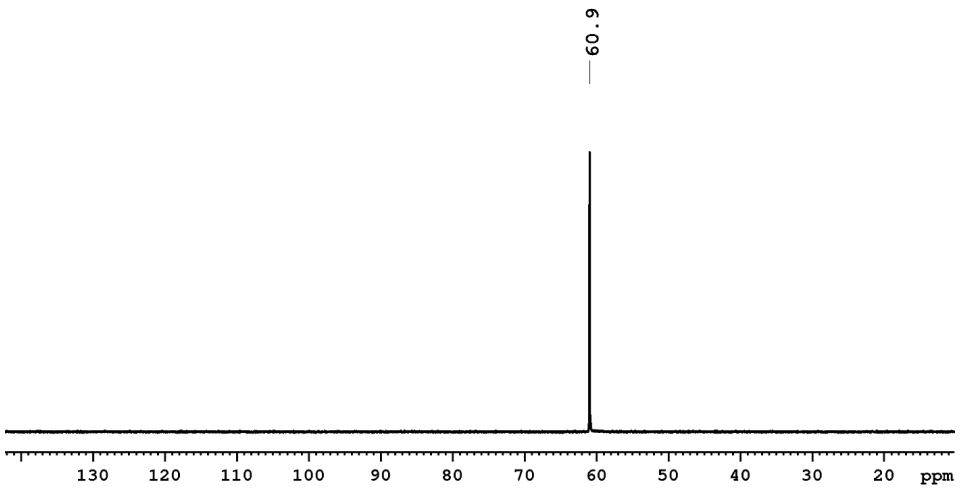

Figure S20. $^{31}P\{^{1}H\}$ NMR spectrum of the complex *fac*-**3b** in $CDCl_3$ (202 MHz).

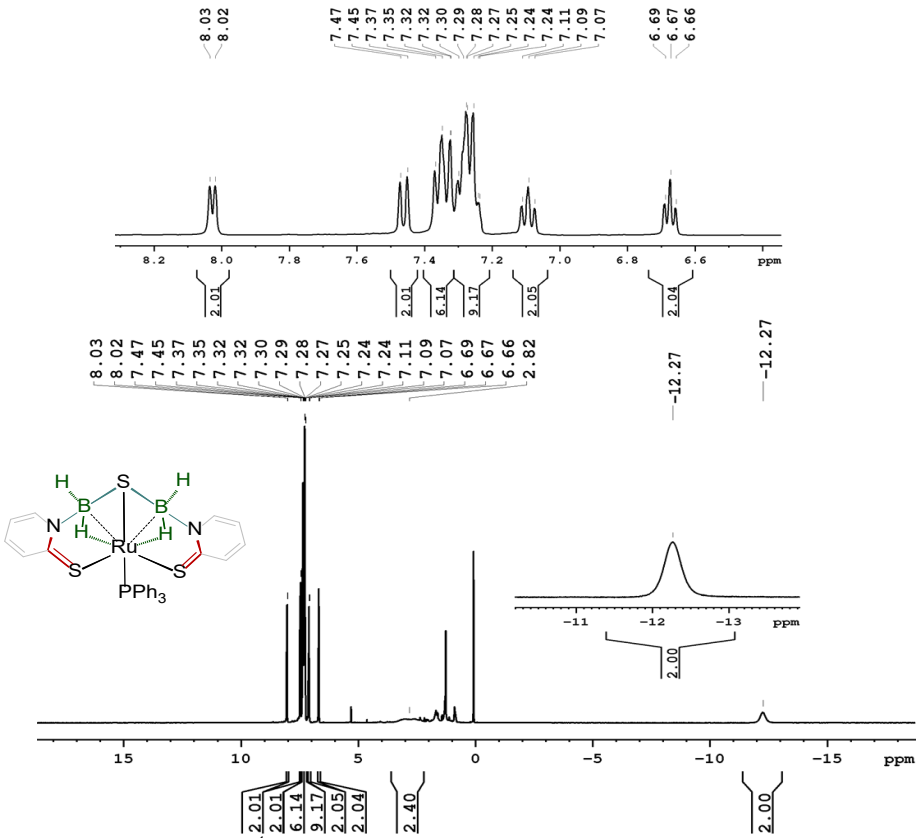

Figure S21. ^{1}H NMR spectrum of the complex *fac*-**3c** in $CDCl_3$ (400 MHz).

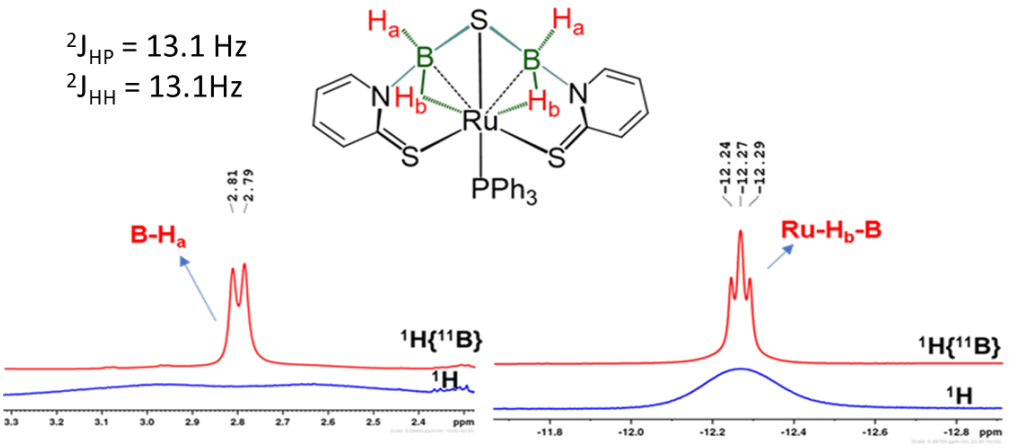

Figure S22. Combined ^{1}H NMR and $^{1}H\{^{11}B\}$ NMR spectra of complex *fac*-**3c** in $CDCl_3$ (500 MHz).

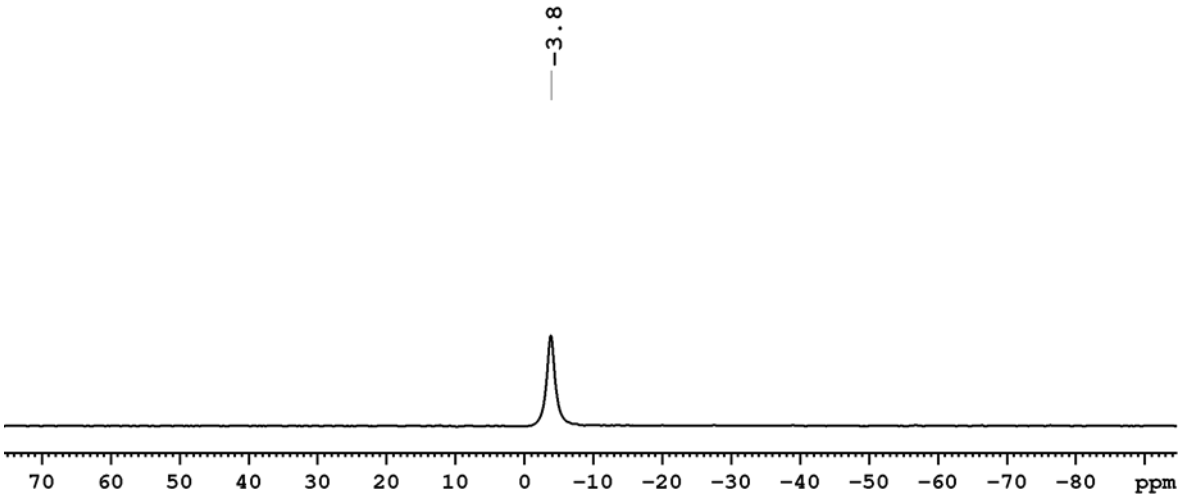

Figure S23. $^{11}B\{^{1}H\}$ NMR spectrum of the complex *fac*-**3c** in $CDCl_3$ (160 MHz).

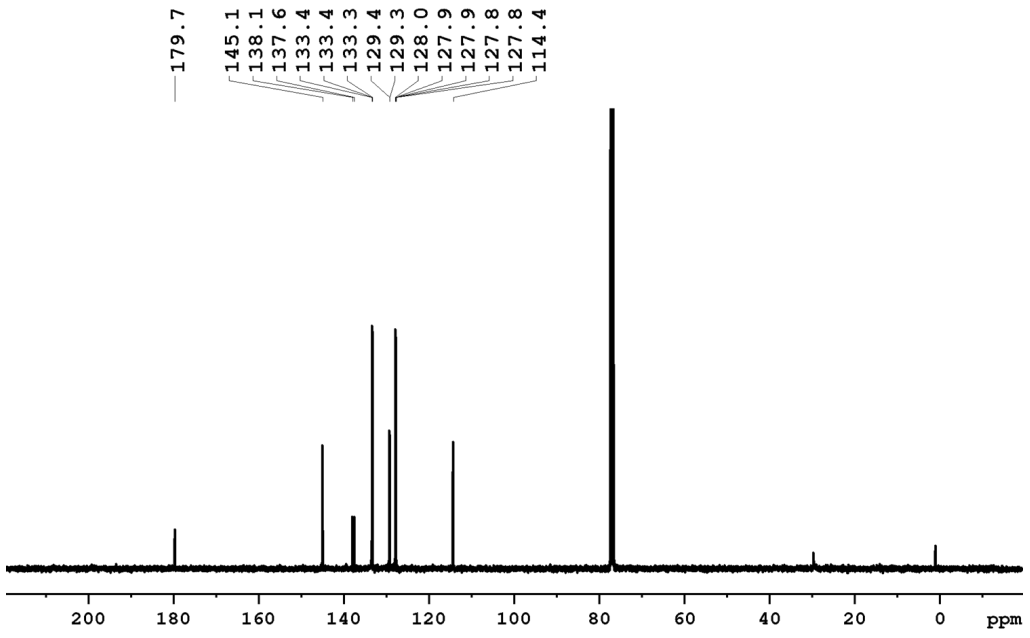

Figure S24. $^{13}C\{^{1}H\}$ NMR spectrum of the complex *fac*-**3c** in $CDCl_3$ (125 MHz). (*=.solvent and grease impurities).

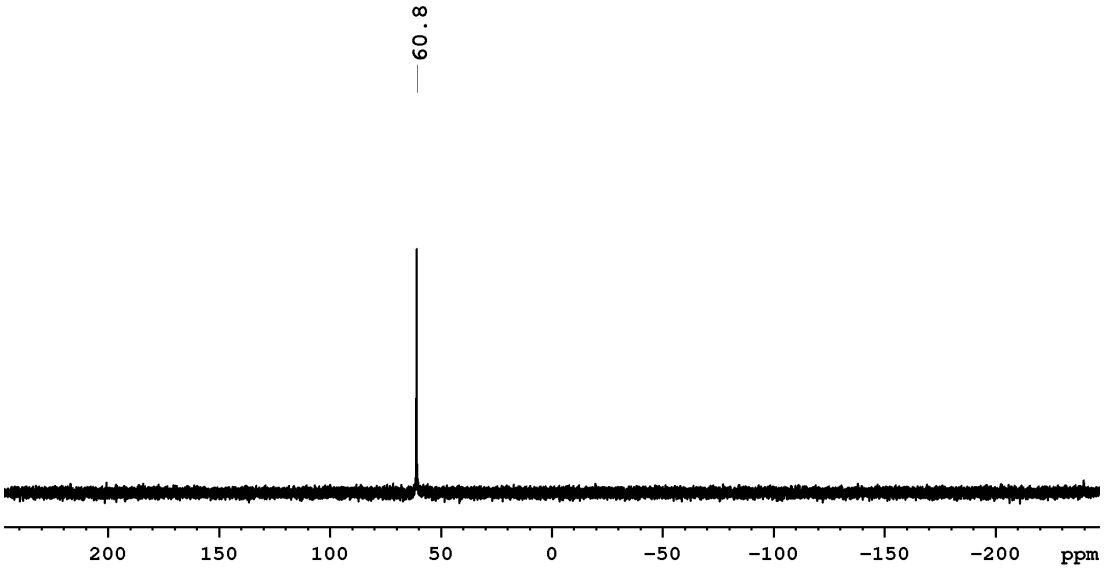

Figure S25. $^{31}P\{^{1}H\}$ NMR spectrum of the complex *fac*-**3c** in $CDCl_3$ (202 MHz).

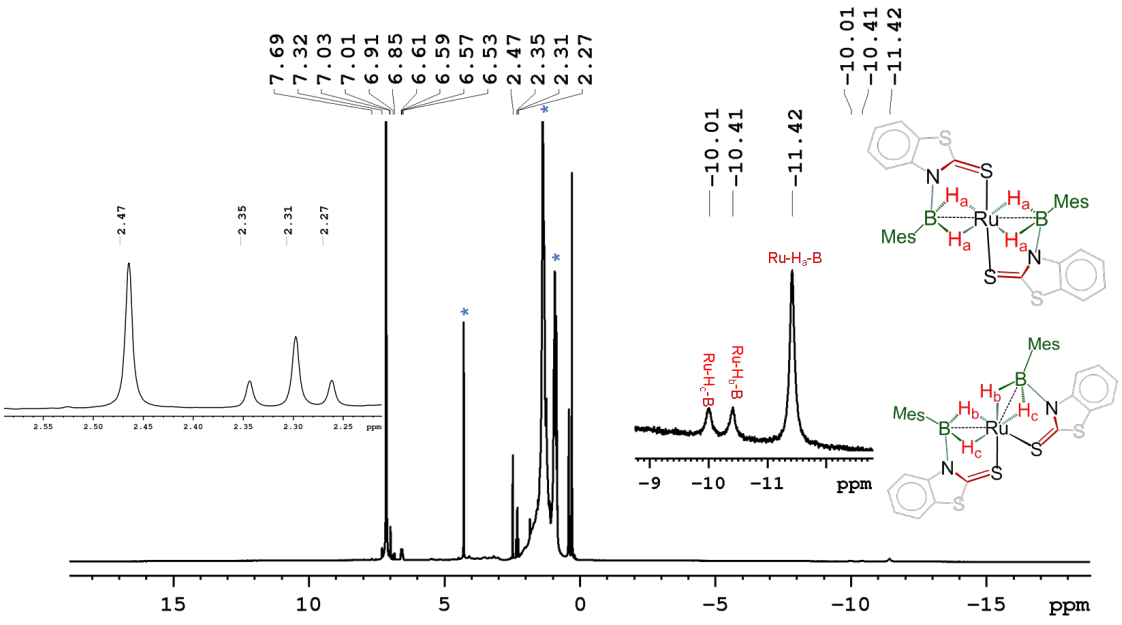

Figure S26. Combined ^{1}H NMR spectrum of the complex *trans*-**4** and *cis*-**4** in Benzene-d_6 (500 MHz) (•=.solvent and grease impurities).

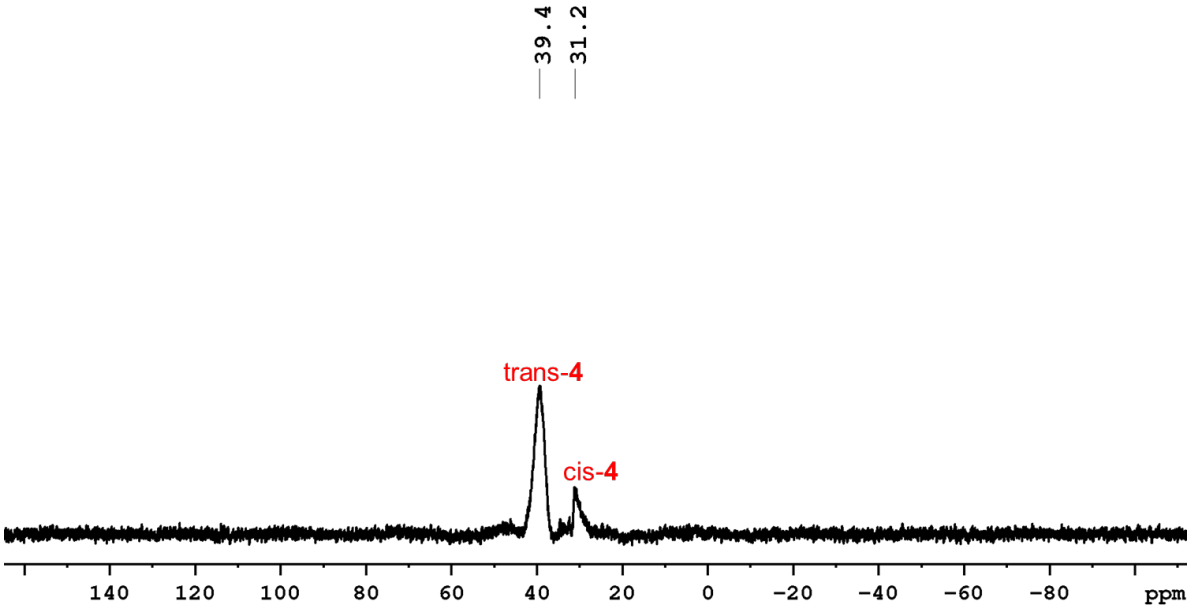

Figure S27. Combined $^{11}B\{^{1}H\}$ NMR spectrum of the complex *trans*-**4** and *cis*-**4** in Toluene-d_8 (160 MHz).

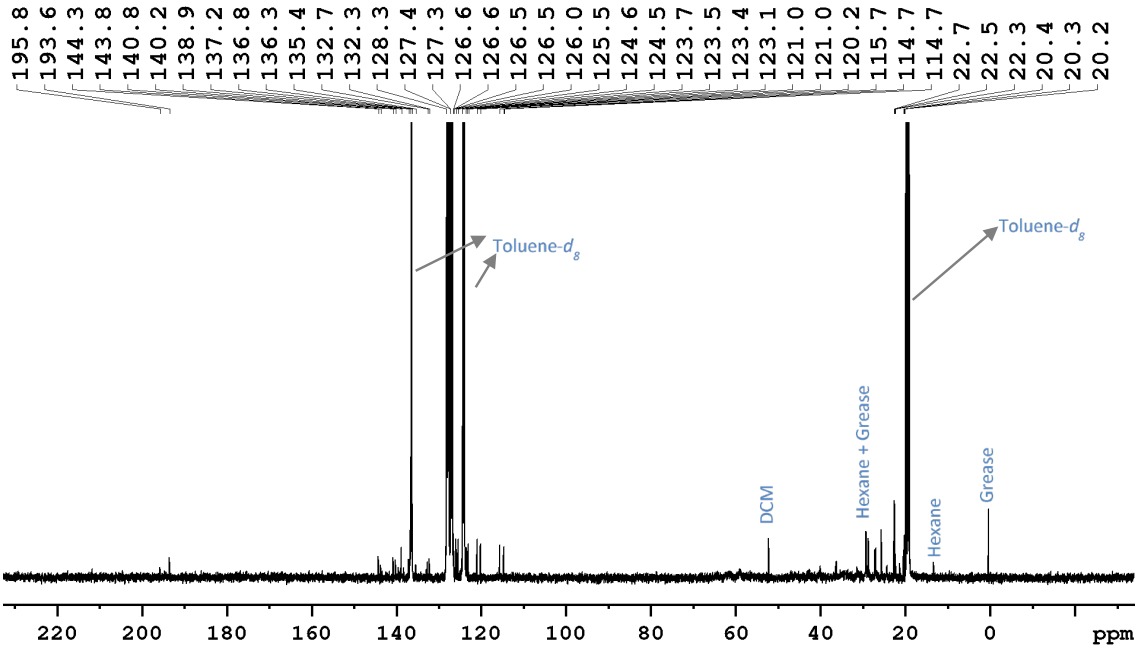

Figure S28. Combined $^{13}C\{^{1}H\}$ NMR spectrum of *trans*-**4** and *cis*-**4** in Toluene-d_8 (125 MHz).

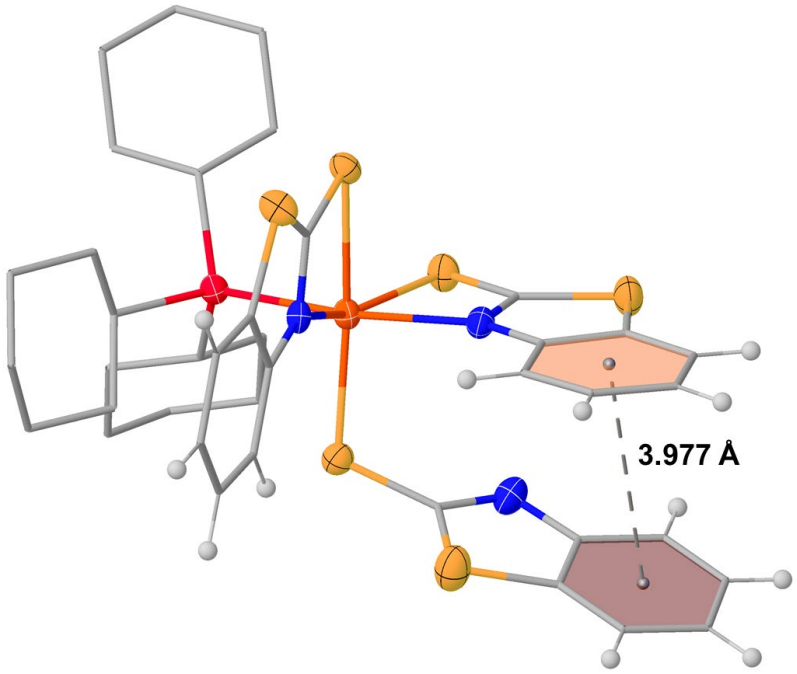

Figure S29. π-π stactking of mercatobenzothiazolyl rings in *mer*-**2a**.

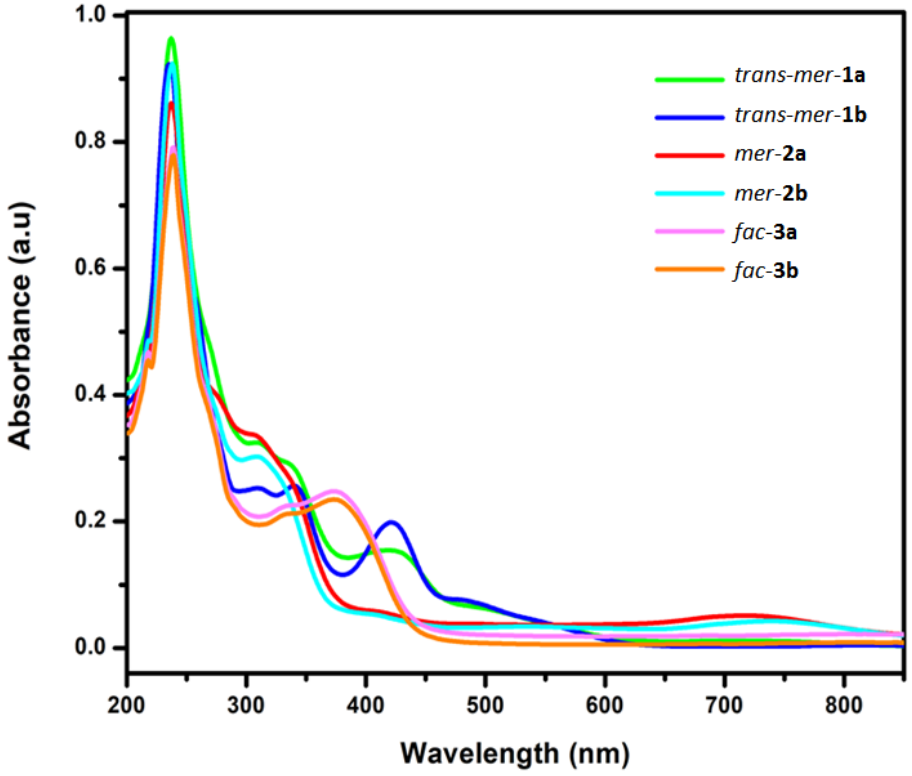

Figure S30. UV-Vis absorption spectra of *trans-mer*-**1a-b**, *mer*-**2a-b** and *fac*-**3a-b** in dicloromethane.

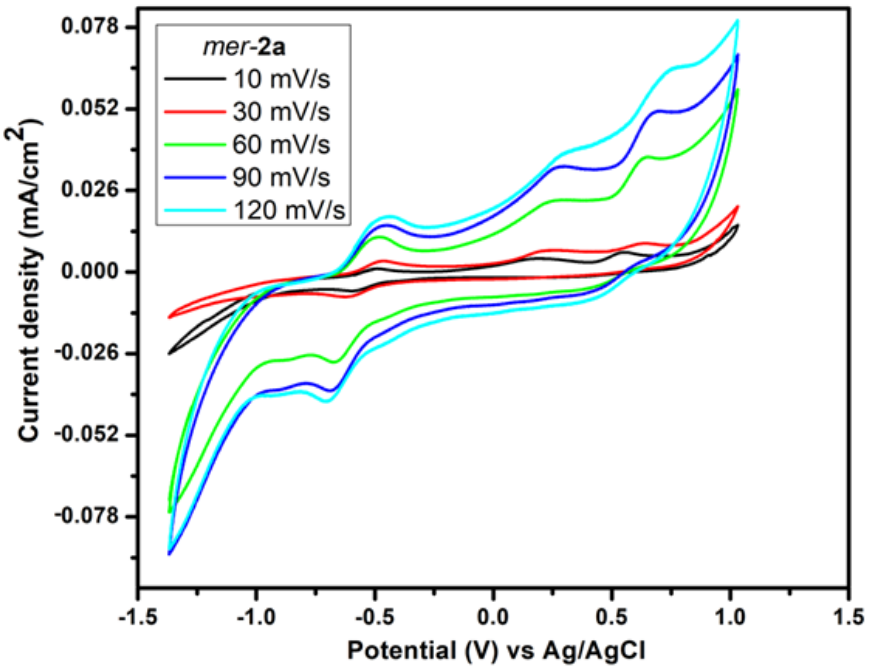

Figure S31. Cyclic voltammetry (CV) curves of complex *mer*-**2a** at different scan rates.

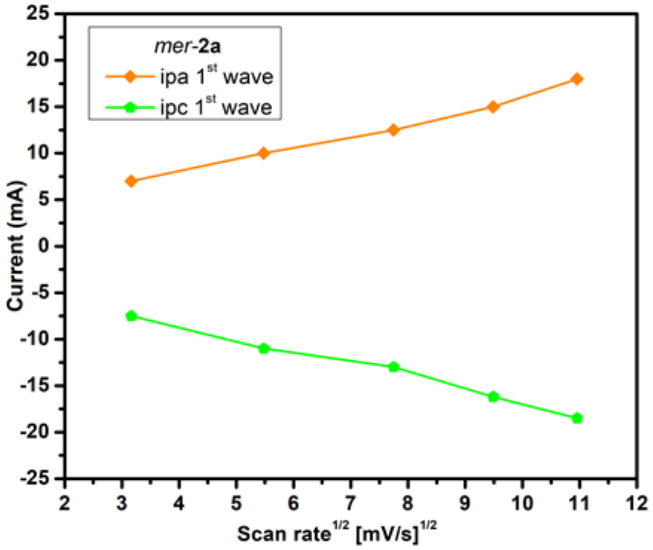

Figure S32 Plot of cathodic and anodic peak current vs square root of scan rate for the first redox reversible wave couple of complex *mer*-**2a.**

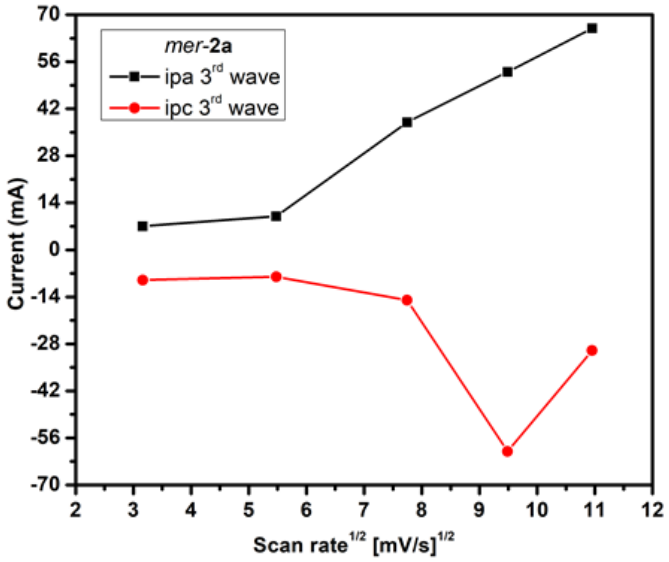

Figure S33. Plot of cathodic and anodic peak current vs square root of scan rate for the third quasi-reversible wave couple of complex *mer*-**2a.**

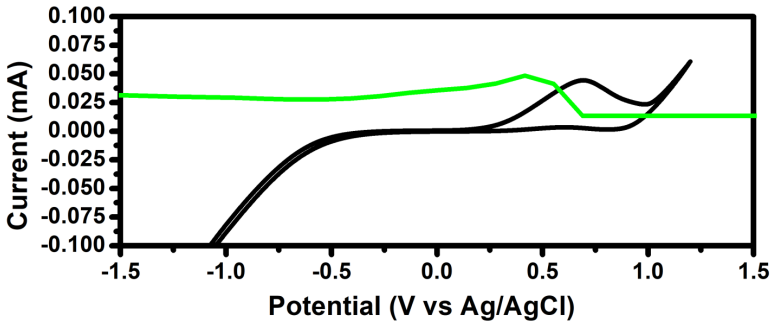

Figure S34. CV of 2-mercaptobenzothiazole.

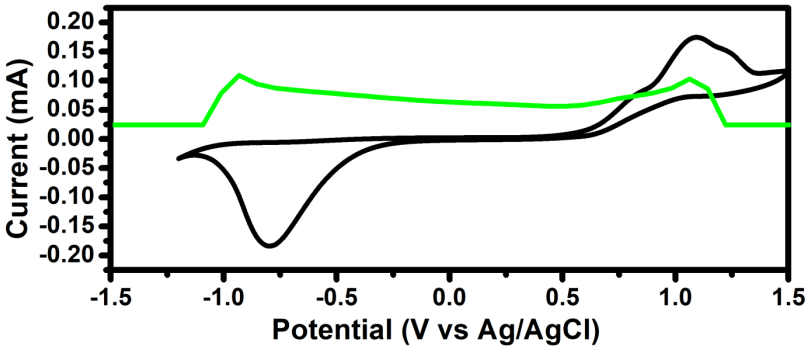

Figure S35. CV of dihydrobis(2-mercaptobenzothiazolyl) borate.

I.3 X-ray analysis details

Suitable X-ray quality crystals of *mer*-**2a**, *fac*-**3a** and *trans*-**4** were grown by slow diffusion of a hexane-CH_2Cl_2 solution at -5 ˚C. Crystal data of *mer*-**2a** and *fac*-**3a** were obtained using a Bruker AXS Kappa APEXII CCD diffractometer with graphite monochromated Mo-Kα (λ = 0.71073 Å) radiation at 296 K and 150 K respectively. The crystal data of *trans*-**4** was collected and integrated using a CMOS D_8 VENTURE Bruker-AXS diffractometer with graphite monochromated Mo-Kα (λ = 0.71073 Å) radiation at 297 K. All the structures were solved using SIR97[5] and refined with SHELXL−2018, SHELXL-2014, and SHELXL-2017[6] Using Olex2[7] all the molecular structures were drawn. The non-hydrogen atoms were refined with anisotropic displacement parameters. All hydrogens could be located in the difference Fourier map. However, the hydrogen atoms bonded to carbons and borons were fixed at chemically meaningful positions and were allowed to ride with the parent atom during the refinement. Crystallographic data have been deposited with the Cambridge Crystallographic Data Center as supplementary publication no CCDC-1875697 (*mer*-**2a**), CCDC-1984218 (*fac*-**3a**), CCDC-2126931 (*fac*-**3c**), CCDC-2040802 (*trans*-**4**). These data can be obtained free of charge from The Cambridge Crystallographic Data Centre via www.ccdc.cam.ac.uk/data_request/cif.

Crystal data for mer-**2a***:* $C_{39}H_{44}N_3PRuS_6$, M_r= 963.16, monoclinic, space group *C1 2/c1*, a = 43.162(6) Å, b = 11.6075(14) Å, c = 17.077(2) Å, α = 90°, β = 94.107(5)°, γ = 90°, V = 8533.5(19) Å^3, Z = 8, ρcalcd = 1.4993 g/cm^3, μ = 0.857 mm^{-1}, F(000) = 3960.0, R_1 = 0.0685, wR_2 = 0.1845, 7512 independent reflections [2θ ≤ 50.000°] and 478 parameters.

Crystal data for fac-**3a***:* $C_{32}H_{45}B_2N_2PRuS_5$, M_r = 771.66, monoclinic, space group *P21/c*, a = 17.2497(13) Å, b = 15.0068(10) Å, c = 19.7663(14) Å, α = 90°, β = 115.089(2)°, γ = 90°, V = 4634.0(6) Å^3, Z = 4, ρcalcd = 1.106 g/cm^3, μ = 0.618 mm^{-1}, F(000) = 1600.0, R_1 = 0.0356, wR_2 = 0.0872, 10624 independent reflections [2θ ≤ 50.486°] and 443 parameters.

*Crystal data for fac-**3c**:* $C_{28}H_{27}B_2N_2PRuS_3$, M_r = 642.03, monoclinic, space group P21/n, a = 9.9824(3) Å, b = 23.4742(9) Å, c = 13.6413(6) Å, α = 90°, β = 94.6068(17)°, γ = 90°, V = 3186.2(2) Å^3, Z = 4, ρcalcd = 1.514 g/cm^3, μ = 0.930 mm^{-1}, F(000) = 1472, R_1 = 0.0338, wR_2 = 0.0740, 5602 independent reflections [2θ ≤ 50.000°] and 377 parameters.

Crystal data for trans-**4***:* $C_{32}H_{36}BCl_2N_2RuS_4$, M_r = 782.47, triclinic, space group *P-1*, a = 8.1421(16) Å, b = 9.0380(16) Å, c = 11.991(2) Å, α = 91.746(5)°, β = 95.358(6)°, γ = 91.618(5)°, V = 877.7(3) Å^3, Z = 1, ρcalcd = 1.480 g/cm^3, μ = 0.863 mm^{-1}, F(000) = 400, R_1 = 0.0486, wR_2 = 0.1206, 3426 independent reflections [2θ ≤ 50.48°] and 217 parameters.

II Computational Details

II.1 Computational details: Density functional theory (DFT) calculations employing B3PW91[8] functional were performed with the Gaussian 09[9] program. Full geometry optimizations were conducted in gaseous state (no solvent effect) without any symmetry constraints using a LANL2DZ[10] basis set on ruthenium and phosphorous atoms and 6-31G(d,p)[11] basis set on remaining atoms (C, H, B, N, S). The optimized geometries were characterized as true minima by conducting frequency calculations. We have computed ^{11}B NMR chemical shifts using gauge-including atomic orbitals (GIAOs)[12] method at the same basis set by B3LYP. The ^{11}B NMR chemical shifts were calculated relative to B_2H_6 and converted to the usual [BF_3.OEt_2] scale by using experimental δ (^{11}B) value of B_2H_6 (δ = 16.6 ppm).[13] Natural bonding analyses were carried out with the natural bond orbital (NBO) 6.0 version of program.[14] Wiberg bond indices (WBI)[15] were obtained from natural bond orbital analysis. The electron density and Laplacian electronic distribution plots were generated using Multiwfn package.[16] All the optimized structures and orbital plots were gerenated by using Chemcraft.[17]

II.2 Computational data

Table S1. Selected geometrical parameters and Wiberg bond indices (WBI) of *mer*-**2a-b**, *fac*-**3a-b**, *trans*-**4** and *cis*-**4**.

mer-**2a**				*mer*-**2b**			
	Expt.	Cal.	WBI		Expt.	Cal.	WBI
Ru1-P1	2.347(2)	2.494	0.516	Ru1-P1	-	2.449	0.498
Ru1-S1	2.278(2)	2.301	0.771	Ru1-S1	-	2.295	0.784
Ru1-S3	2.491(2)	2.535	0.402	Ru1-S3	-	2.540	0.402
Ru1-S6	2.342(2)	2.406	0.634	Ru1-S6	-	2.401	0.631
Ru1-N1	2.138(6)	2.167	0.314	Ru1-N1	-	2.160	0.320
Ru1-N2	2.164(6)	2.123	0.340	Ru1-N2	-	2.112	0.349
C1-S1	1.740(9)	1.745	1.134	C1-S1	-	1.743	1.142
C8-S6	1.711(8)	1.718	1.220	C8-S6	-	1.722	1.217
fac-**3a**				*fac*-**3b**			
	Expt.	Cal.	WBI		Expt.	Cal.	WBI
Ru1-B1	2.293(3)	2.308	0.218	Ru1-B1	-	2.304	0.218
Ru1-B2	2.276(2)	2.293	0.228	Ru1-B2	-	2.306	0.217
Ru1-H1B	1.69(3)	1.703	0.241	Ru1-H1B	-	1.706	0.240
Ru1-H2B	1.69(3)	1.698	0.245	Ru1-H2B	-	1.702	0.241
B1-H1B	1.29(3)	1.363	0.578	B1-H1B	-	1.360	0.581
B2-H2B	1.37(3)	1.370	0.571	B2-H2B	-	1.363	0.578
B1-S5	1.914(3)	1.925	0.984	B1-S5	-	1.929	0.976
Ru1-P1	2.3071(6)	2.416	0.503	Ru1-P1	-	2.393	0.488
Ru1-S5	2.4184(6)	2.436	0.369	Ru1-S5	-	2.427	0.383
trans-**4**				*cis*-**4**			
	Expt.	Cal.	WBI		Expt.	Cal.	WBI
Ru1-B1	2.172	2.173	0.369	Ru1-B1	-	2.149	0.368
Ru1-H1	1.60(4)	1.727	0.248	Ru1-H1	-	1.723	0.245
Ru1-H2	1.62(4)	1.727	0.248	Ru1-H2	-	1.743	0.214
B1-H1	1.35(4)	1.357	0.597	B1-H1	-	1.371	0.590
B1-H2	1.33(4)	1.357	0.597	B1-H2	-	1.360	0.624
Ru-S1	2.3221(10)	2.365	0.465	Ru-S1	-	2.365	0.512
B1-C1	1.580(5)	1.589	0.895	B1-C1	-	1.589	0.892

Table S2. Calculated natural charges (q), natural valence population (Pop) and HOMO – LUMO gaps of *mer*-**2a-b**, *fac*-**3a-b**, *trans*-**4** and *cis*-**4**.

Compound	q_{Ru1}	q_{N1}	q_{S3}	q_{S1}	q_{S6}	**Pop(Ru_{val})**	**Pop(N_{val})**	**Pop(S_{val})**	**ΔE_{H-L} (eV)**
mer-**2a**	0.171	-0.516	-0.027	0.047	0.064	7.788	5.487	5.994	2.053
mer-**b**	0.136	-0.511	-0.034	0.086	0.066	7.822	5.481	6.002	1.995
Compound	q_{Ru}	q_B	q_S	q_P	**Pop(Ru_{val})**	**Pop(B_{val})**	**Pop(S_{val})**	**Pop(P_{val})**	**ΔE_{H-L} (eV)**
fac-**3a**	-0.429	0.029	0.070	1.131	8.408	2.945	5.893	3.849	3.870
fac-**3b**	-0.432	0.028	0.075	1.156	8.410	2.945	5.889	3.823	3.952
trans-**4**	-0.340	0.338	0.138	-	8.317	2.631	5.824	-	3.143
cis-**4**	-0.330	0.333	0.149	-	8.313	2.637	5.813	-	3.625

Table S3. Experimentally observed and calculated ^{11}B chemical shifts of *fac*-**3a-b**, *trans*-**4** and *cis*-**4**.

Molecule		**^{11}B NMR**	
		Exp.	Cal.
fac-**3a**	B	-10.1	-10.1
fac-**3b**	B	-11.5	-10.8
trans-**4**	B	37.4	33.5
cis-**4**	B	30.3	30.2

Table S4. Topological parameters at selected bond critical points (BCPs) in *mer*-**2a-b**, *fac*-**3a-b**, *trans*-**4** and *cis*-**4**.

Molecule	BCP	ρ	H	$\nabla^2\rho$	*ELF*	ε
mer-**2a**	Ru1-P1	0.064	-0.014	0.169	0.213	0.464
	Ru1-S1	0.198	-0.167	-0.463	0.934	0.069
	Ru1-N1	0.053	-0.003	0.400	0.042	1.328
	Ru1-S6	0.075	-0.020	0.163	0.281	0.345
mer-**2b**	Ru1-P1	0.067	-0.014	0.200	0.193	1.721
	Ru1-S1	0.086	-0.019	0.272	0.234	0.351
	Ru1-N1	0.025	-0.002	0.141	0.026	3.414
	Ru1-S6	0.074	-0.019	0.172	0.266	0.399
fac-**3a**	Ru1-P1	0.074	-0.020	0.185	0.241	0.142
	Ru1-S1	0.074	-0.019	0.205	0.219	0.539
	Ru1-S3	0.074	-0.020	0.192	0.233	0.591
	Ru1-S5	0.046	-0.007	0.220	0.069	4.716
	S5-B1	0.114	-0.106	-0.194	0.647	0.050
	S5-B2	0.124	-0.118	-0.230	0.685	0.141
	Ru1-H1B	0.068	-0.011	0.645	0.034	1.704
	B1-H1B	0.055	-0.027	0.362	0.037	0.031
fac-**3b**	Ru1-P1	0.076	-0.019	0.224	0.212	0.045
	Ru1-S1	0.075	-0.019	0.204	0.225	0.476
	Ru1-S3	0.075	-0.019	0.204	0.226	0.455
	S5-B1	0.116	-0.109	-0.171	0.591	0.162
	S5-B2	0.116	-0.108	-0.167	0.583	0.163
	Ru1-H1B	0.053	-0.009	0.304	0.619	2.123
	B1-H1B	0.143	-0.146	-0.269	0.670	0.189
trans-**4**	Ru1-S1	0.288	-0.300	-0.102	0.985	0.022
	Ru1-H1	0.081	-0.025	0.482	0.082	0.131
	Ru1-H2	0.081	-0.025	0.482	0.082	0.131
	B1-H1	0.151	-0.160	-0.319	0.698	0.049
	B1-H2	0.151	-0.160	-0.319	0.698	0.049
cis-**4**	Ru1-S1	0.085	-0.023	0.189	0.306	0.182
	Ru1-S2	0.085	-0.023	0.188	0.306	0.182
	Ru1-H2	0.063	-0.015	0.301	0.090	0.488
	B1-H1	0.145	-0.153	-0.324	0.720	0.204
	B2-H2	0.147	-0.154	-0.329	0.726	0.199

Electron density, ρ, Total energy density, H, Laplacian of the electron density, $\nabla^2\rho$, Electron localization function, *ELF*, Ellipticity, ε in a.u.

Table S5. Electronic transition configurations for *mer*-**2a-b** by TD-DFT calculations.

Compounds	Excited state	Major transition configurations
mer-**2a**	1	HOMO-6(B)->LUMO(B) (18%), HOMO-5(B)->LUMO(B) (12%), HOMO-3(B)->LUMO(B) (10%)
	2	HOMO-8(B)->LUMO(B) (21%), HOMO-5(B)->LUMO(B) (25%), HOMO-3(B)->LUMO(B) (35%)
	3	HOMO(B)->LUMO(B) (88%)
	4	HOMO-2(B)->LUMO(B) (50%), HOMO-1(B)->LUMO(B) (24%)
	5	HOMO-7(A)->LUMO(A) (11%), HOMO-1(A)->LUMO(A) (11%), HOMO-6(B)->LUMO+1(B) (10%)
	6	HOMO-5(B)->LUMO+1(B) (12%), HOMO-3(B)->LUMO+1(B) (12%)
	7	HOMO(A)->LUMO(A) (49%), HOMO-25(A)->LUMO(A) (4%)
	8	HOMO-7(B)->LUMO(B) (13%), HOMO-5(B)->LUMO(B) (10%), HOMO-3(B)->LUMO(B) (16%)
	9	HOMO-7(B)->LUMO(B) (20%), HOMO-6(B)->LUMO(B) (51%)
	10	HOMO-7(A)->LUMO+2(A) (11%), HOMO-1(A)->LUMO+2(A) (10%), HOMO-1(B)->LUMO+4(B) (12%)
mer-**2b**	1	HOMO-2(B)->LUMO(B) (14%), HOMO-1(B)->LUMO(B) (28%)
	2	HOMO-11(B)->LUMO(B) (21%), HOMO-9(B)->LUMO(B) (13%), HOMO-5(B)->LUMO(B) (23%)
	3	HOMO(B)->LUMO(B) (89%)
	4	HOMO-2(B)->LUMO(B) (42%), HOMO-1(B)->LUMO(B) (31%)
	5	HOMO-1(A)->LUMO(A) (11%), HOMO-1(B)->LUMO+1(B) (16%)
	6	HOMO-4(B)->LUMO(B) (16%), HOMO-1(B)->LUMO(B) (20%)
	7	HOMO(A)->LUMO(A) (56%), HOMO-25(A)->LUMO(A) (4%)
	8	HOMO-8(B)->LUMO(B) (22%), HOMO-6(B)->LUMO(B) (37%), HOMO-2(B)->LUMO(B) (13%)
	9	HOMO-5(B)->LUMO+1(B) (11%)
	10	HOMO-19(A)->LUMO+1(A) (2%)

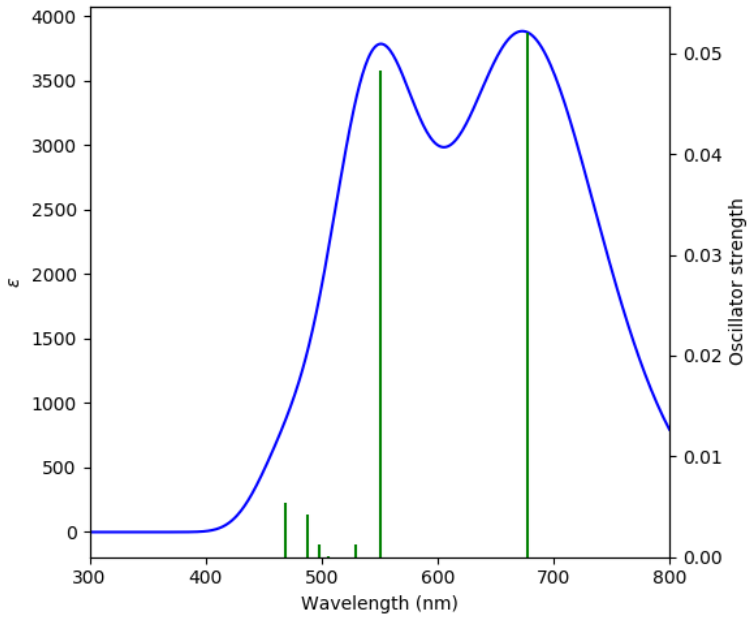

Figure S36. Calculated UV-Vis absorption spectra of *mer*-**2a** at CAM-B3LYP/LANL2DZ/6-31G(d,p) level.

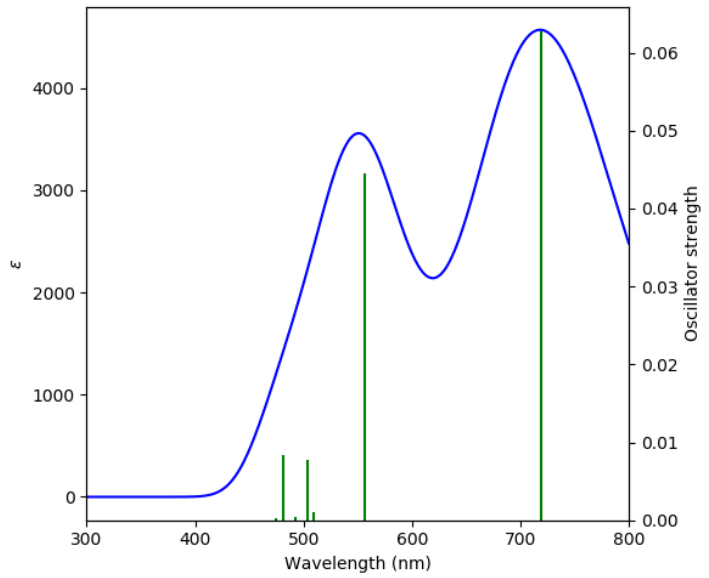

Figure S37. Calculated UV-Vis absorption spectra of *mer*-**2b** at CAM-B3LYP/LANL2DZ/6-31G(d,p) level.

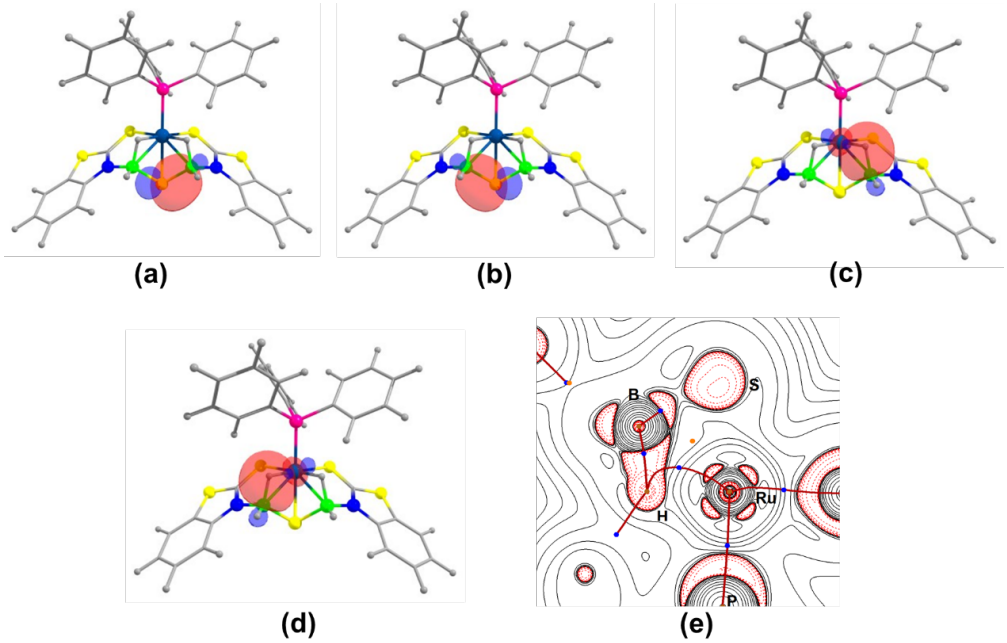

Figure S38. Natural bond orbital interaction between B-S bond (a,b) and B-H-Ru (c,d) in *fac*-**3b** (isovalue ±0.04 [e/bohr^3]$^{1/2}$); (e) Contour-line map of the Laplacian of the electron density in the Ru-H-B plane of *fac*-**3a**.

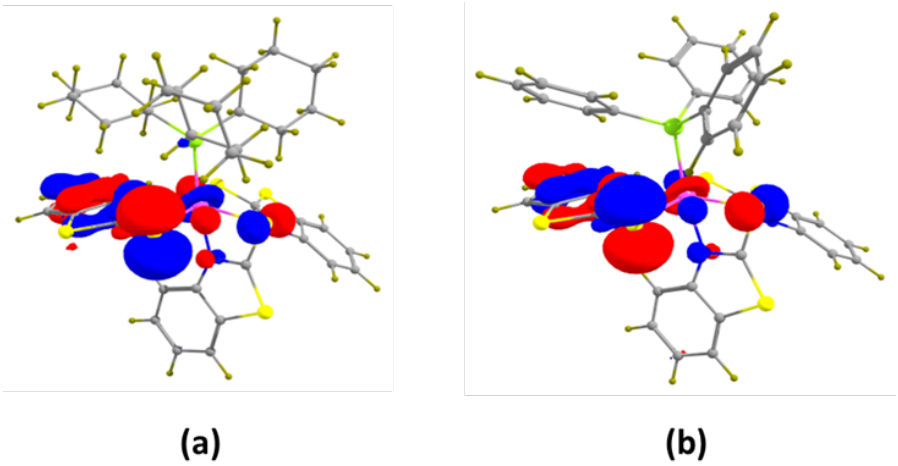

Figure S39. (a) HOMO of oxidised form of *mer*-**2a** and (b) HOMO of oxidised form of *mer*-**2a**.

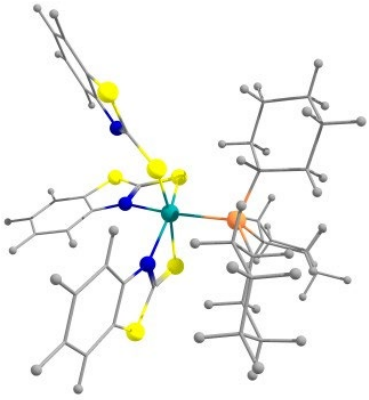

Figure S40. Optimized geometry of *mer*-**2a**.

Cartesian coordinates for the calculated structure of *mer*-**2a** (in Å).

C	-2.46501900	-1.23244600	-1.34277100	C	-3.93173500	3.72554300	0.86062000
C	-4.48878600	-1.84261700	-0.69836500	H	-4.01675900	4.62254200	0.25435500
C	-5.55474300	-2.08881000	0.17848600	C	-4.90338000	3.45531000	1.83421800
H	-5.42542300	-1.88686900	1.23680900	H	-5.73069600	4.14428500	1.97614900
C	-6.74598900	-2.58529600	-0.33034300	C	-4.82530000	2.31088000	2.62257500
H	-7.57708600	-2.77976300	0.34153300	H	-5.58015000	2.10028800	3.37376800
C	-6.89366100	-2.84114800	-1.70268500	C	-3.75377300	1.44393600	2.42034100
H	-7.83578700	-3.22977500	-2.07877900	C	1.03990500	2.64949700	0.93008000
C	-5.84989300	-2.60537000	-2.59129100	C	0.44535600	3.01182200	-1.21934300
H	-5.96775500	-2.80558100	-3.65174100	C	-0.07114700	2.76445800	-2.49708500
C	-4.65093400	-2.10654400	-2.08141900	H	-0.43748400	1.77331600	-2.74338300
C	-1.97725300	-0.23646800	2.23936300	C	-0.11356000	3.80840800	-3.41434300
C	-2.76805100	1.71360600	1.44390200	H	-0.51463600	3.62586400	-4.40698000
C	-2.86162700	2.86442400	0.65562200	C	0.34582400	5.08892700	-3.07943300
H	-2.11020800	3.06165600	-0.10069900	H	0.30340600	5.88772600	-3.81377800

C	0.84933900	5.35332800	-1.80852200
H	1.19572100	6.34736000	-1.54311600
C	0.89034700	4.31208700	-0.88383800
C	2.02245300	-2.64716700	-0.80830800
H	1.41942400	-2.38223800	-1.68839200
C	1.16529800	-3.59755600	0.03527600
H	0.24931200	-3.09506600	0.35707700
H	1.71203400	-3.89022200	0.94113600
C	0.80677900	-4.85704300	-0.76221000
H	0.21803000	-5.53403600	-0.13202800
H	0.15847800	-4.57324400	-1.60276000
C	2.05035100	-5.56864300	-1.29644900
H	1.76509400	-6.43571600	-1.90422100
H	2.63712800	-5.95871400	-0.45211700
C	2.92102000	-4.61110400	-2.11078600
H	2.37928600	-4.30699000	-3.01756400
H	3.83607400	-5.11362000	-2.44744500
C	3.28855500	-3.36055500	-1.30060100
H	3.90183300	-3.66781200	-0.44422500
H	3.90979000	-2.69988600	-1.91461000
C	3.44282800	-0.99934000	1.50542800
H	3.47326000	0.05953200	1.79740000
C	2.85267400	-1.76788800	2.69244100
H	1.83179400	-1.43225900	2.89645400
H	2.79647900	-2.83735100	2.45098000
C	3.72180500	-1.58289500	3.94175200
H	3.29679700	-2.15584600	4.77436300
H	3.69235100	-0.52639700	4.24254700
C	5.17146600	-1.99988900	3.68964100
H	5.78549700	-1.80888100	4.57795000
H	5.21165500	-3.08407000	3.51038900
C	5.75097800	-1.26915900	2.47742900
H	6.77129100	-1.61524700	2.27156400
H	5.82453200	-0.19527100	2.70046800
C	4.87906400	-1.46289900	1.22917300
H	5.32293100	-0.92086100	0.38793400
H	4.88089800	-2.52489700	0.95716500
C	3.36042800	-0.03629400	-1.32104700
H	4.22545900	-0.70163100	-1.44884700
C	2.65654900	0.08489700	-2.67723600
H	2.30630400	-0.89272300	-3.02642000
H	1.76677200	0.71474500	-2.56409500
C	3.58967100	0.69889700	-3.72802700
H	4.42317000	0.00714400	-3.91812600
H	3.05288700	0.80656700	-4.67815100
C	4.14658200	2.04856800	-3.27253100
H	3.32420400	2.77313900	-3.20159500
H	4.84834900	2.44190500	-4.01796400
C	4.83031600	1.92813100	-1.90962300
H	5.72253300	1.29203500	-2.00404500
H	5.18256800	2.90920200	-1.56925300
C	3.88862900	1.32717300	-0.85924600
H	3.04498600	2.00590400	-0.69963200
H	4.41092400	1.24323300	0.09973100
N	0.57209100	2.10585700	-0.18138000
N	-1.78923900	0.74518600	1.38391400
N	-3.25520900	-1.35475300	-0.32262800
P	2.26356500	-0.90864600	-0.01240500
S	-0.80151300	-0.70666400	-1.39664700
S	-3.17418300	-1.71240900	-2.91448100
S	1.14631200	1.63251200	2.29858400
S	1.43046100	4.35560800	0.78384900
S	-3.39689100	-0.06342400	3.24506100
S	-0.76637700	-1.45408700	2.16513600
Ru	0.07033200	0.13238700	0.56090500

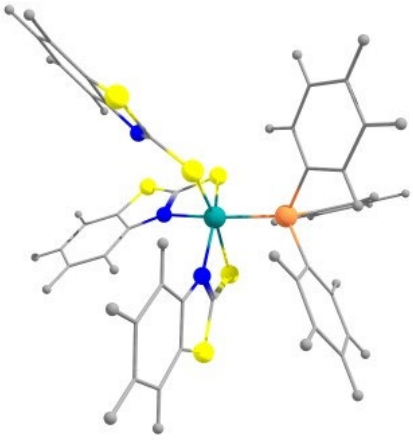

Figure S41. Optimized geometry of *mer*-**2b**.

Cartesian coordinates for the calculated structure of *mer*-**2b** (in Å).

C	2.47270800	-1.20418000	1.31051200
C	4.54184800	-1.65332400	0.67771800
C	5.62574000	-1.82920800	-0.19458600
H	5.47956200	-1.66723200	-1.25755700
C	6.85521400	-2.20677500	0.32471300
H	7.70040500	-2.34603500	-0.34327200
C	7.02403200	-2.41233100	1.70332000
H	7.99638200	-2.70706300	2.08766800
C	5.96360200	-2.24487200	2.58749100
H	6.09824900	-2.40565900	3.65263100
C	4.72569800	-1.86590100	2.06724100
C	1.92074900	-0.22186100	-2.24184900
C	2.62187800	1.74557700	-1.40203800
C	2.65709000	2.88384900	-0.59135900
H	1.89224000	3.03039700	0.16344200
C	3.68605500	3.79804000	-0.77598800
H	3.72700900	4.68685400	-0.15333400
C	4.67200100	3.59233200	-1.75130100
H	5.46604500	4.32237600	-1.87702000
C	4.65008800	2.46171400	-2.56281600
H	5.41544400	2.30274800	-3.31606100
C	3.62007800	1.54155700	-2.38128700
C	-1.30225600	2.48760800	-0.74636800
C	-0.76609500	2.70028000	1.43684000
C	-0.26217700	2.37663600	2.70176700
H	0.18079800	1.40026400	2.86651600
C	-0.33684200	3.32693300	3.71368200
H	0.05471500	3.08551100	4.69762400
C	-0.90292100	4.58808300	3.48578300
H	-0.94895500	5.31404100	4.29215700
C	-1.40401300	4.92543200	2.23137800
H	-1.83890300	5.90362000	2.05056400
C	-1.32970300	3.97777200	1.21319100
N	-0.78085800	1.89449000	0.31256300
N	1.69039300	0.73153400	-1.36526800
N	3.27135000	-1.28531500	0.29160100
P	-2.29538100	-1.03028400	-0.10360100
S	0.76892400	-0.83745500	1.35337300
S	3.22065800	-1.58016200	2.89248800
S	-1.30819200	1.58771900	-2.19931200
S	-1.85976500	4.12431900	-0.45113000
S	3.33259700	0.03729100	-3.23906500
S	0.75334200	-1.48750400	-2.20349400
Ru	-0.13679000	0.03046800	-0.56902600
C	-3.59246000	0.13561600	0.57644300
C	-3.43618000	0.65495100	1.86667400
C	-4.67892400	0.54173700	-0.20174100
C	-4.37023300	1.55153100	2.37989900
H	-2.58400500	0.36196500	2.47319400
C	-5.60863600	1.44520200	0.31300700
H	-4.79780200	0.15694400	-1.20921500
C	-5.45982500	1.94680200	1.60393600
H	-4.23933400	1.94698100	3.38303100
H	-6.44966800	1.75628800	-0.30042800
H	-6.18660400	2.64878200	2.00335100
C	-3.15773300	-1.83425600	-1.57194400
C	-2.73637500	-1.59566700	-2.88072800
C	-4.24514300	-2.68722000	-1.34398300
C	-3.39727300	-2.19949200	-3.95138600
H	-1.88588700	-0.95021800	-3.06477200
C	-4.90545300	-3.28414200	-2.41437000
H	-4.57247800	-2.89299900	-0.32903500
C	-4.48242000	-3.04071600	-3.72140600
H	-3.05582700	-2.00998000	-4.96501800
H	-5.74765300	-3.94425700	-2.22591300
H	-4.99541700	-3.51057600	-4.55613900
C	-2.27643500	-2.47347700	1.10259400
C	-1.29463000	-3.45410200	0.92272000
C	-3.22804600	-2.62873900	2.11298300
C	-1.26784100	-4.57644200	1.74593700
H	-0.54526000	-3.33451900	0.14555200
C	-3.19336300	-3.75217700	2.94067800
H	-3.99739500	-1.87710900	2.25923300
C	-2.21509800	-4.72634900	2.75879700
H	-0.49959000	-5.33035100	1.59962600
H	-3.93550100	-3.86217500	3.72675700
H	-2.18854300	-5.59971100	3.40461900

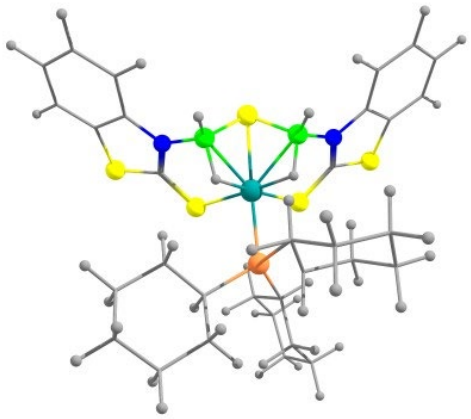

Figure S42. Optimized geometry of *fac*-**3a**.

Cartesian coordinates for the calculated structure of *fac*-**3a** (in Å).

Ru	0.00038000	-0.38059300	-0.27334900	C	3.66957300	-2.98314700	0.27822000
S	-1.77483000	-0.12654300	-1.88174600	C	-0.94938200	2.44942200	1.76524100
S	-4.52432200	-1.35235900	-1.92354300	H	-0.76224300	3.51593300	1.95052500
S	1.77706600	-0.31800700	-1.89501200	C	-2.44894200	2.26155300	1.50152200
S	4.35138700	-1.88343900	-1.97013000	H	-2.63802900	1.21503500	1.22881600
P	0.10109600	1.98036400	0.23337800	H	-2.77124600	2.86777600	0.64773300
N	-2.82128700	-1.80640200	-0.03516800	C	-3.28251700	2.63034800	2.73440100
N	2.63622600	-2.10233600	-0.05050700	H	-3.17816700	3.70708100	2.93231200
C	-2.95118200	-1.11978600	-1.18707600	H	-4.34483300	2.45436300	2.52644700
C	-4.99948100	-2.42663700	-0.62517000	C	-2.84165300	1.84659800	3.97129400
C	-6.20637300	-3.09996100	-0.45746300	H	-3.42613800	2.15469200	4.84663400
H	-7.00915700	-2.99080400	-1.17984400	H	-3.04814400	0.77848200	3.81545200
C	-6.35365800	-3.91892300	0.65859900	C	-1.34690500	2.03607500	4.23304900
H	-7.28589800	-4.45458100	0.80993400	H	-1.02899800	1.43579700	5.09402700
C	-5.30981100	-4.06062500	1.57972200	H	-1.15460100	3.08629700	4.49696400
H	-5.43884600	-4.70953900	2.44079700	C	-0.51196900	1.65804200	3.00475900
C	-4.10305100	-3.38915300	1.41289200	H	-0.62291900	0.58615400	2.79963000
H	-3.29171700	-3.50451900	2.12169700	H	0.55111600	1.82246900	3.21357500
C	-3.95030100	-2.55722800	0.30095900	C	-0.62605900	3.08929800	-1.15881900
H	-1.68224000	-2.05154900	1.93376300	H	-1.63287900	2.66767700	-1.28287100
H	-1.17779800	-0.46706100	0.95334100	C	-0.76243400	4.58376000	-0.84483700
H	1.15121400	-0.57677600	0.96067400	H	-1.28555600	4.74591900	0.10462600
H	1.49035600	-2.21038500	1.92759200	H	0.23539500	5.03034700	-0.74132700
C	2.83132800	-1.44990500	-1.21349400	C	-1.50335400	5.30929000	-1.97601300
C	4.71127400	-2.99419700	-0.66518900	H	-2.52919900	4.92013600	-2.04198200
C	5.82784400	-3.81066700	-0.50704900	H	-1.58869400	6.37701100	-1.73934700
H	6.62571100	-3.81009300	-1.24297900	C	-0.79755900	5.11283600	-3.31877600
C	5.89101900	-4.62904300	0.61740800	H	-1.36296700	5.60040200	-4.12201900
H	6.75191900	-5.27479300	0.76153600	H	0.18432600	5.60690700	-3.28471400
C	4.85341000	-4.62911300	1.55619800	C	-0.60574600	3.62716200	-3.62772100
H	4.91537500	-5.27901900	2.42395400	H	-0.04454900	3.49888900	-4.56088900
C	3.73672300	-3.81496900	1.39866700	H	-1.58642400	3.15783500	-3.78648500
H	2.92986100	-3.82082500	2.12171900	C	0.11300900	2.89466700	-2.48829300

H	1.13968400	3.27831200	-2.40389900	H	4.04589400	3.33283100	3.09290300
H	0.19664500	1.83070700	-2.72918800	H	5.27409400	4.05044400	2.05707400
C	1.83993300	2.74635900	0.57506000	C	3.23890500	4.61193300	1.55580700
H	2.16929500	3.05176400	-0.42844100	H	3.53002700	4.97279400	0.55890200
C	2.85661800	1.72468300	1.09716200	H	3.21560700	5.49167200	2.21069800
H	2.87298300	0.85066300	0.44276000	C	1.83852700	3.99000100	1.47706900
H	2.54693800	1.36947300	2.08962700	H	1.52484000	3.70666200	2.49032700
C	4.25836700	2.33808600	1.18984300	H	1.12204700	4.73847400	1.12713300
H	4.96080100	1.59503100	1.58617500	S	-0.13513800	-2.80700700	-0.10188600
H	4.60687400	2.58504700	0.17672200	B	1.33918800	-1.92108600	0.77234600
C	4.27365900	3.60123200	2.05124200	B	-1.50578400	-1.77922800	0.77727400

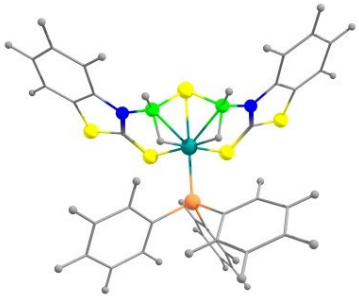

Figure S43. Optimized geometry of *fac*-**3b**.

Cartesian coordinates for the calculated structure of *fac*-**3b** (in Å).

Ru	-0.00751700	-0.30484400	-0.20101300	H	1.57137900	-2.05656500	2.01702100
S	-1.80206500	-0.11335400	-1.78946300	C	2.89032400	-1.21880500	-1.10992200
S	-4.47755800	-1.49198100	-1.82865500	C	4.85956200	-2.63610000	-0.53818900
S	1.76848900	-0.17170100	-1.81507600	C	6.02639800	-3.37548600	-0.36490500
S	4.44829400	-1.54244500	-1.84208600	H	6.83506700	-3.31539900	-1.08646000
P	0.02706900	2.04556900	0.24808800	C	6.12583800	-4.19547600	0.75570900
N	-2.75221900	-1.85035100	0.06036600	H	7.02615500	-4.78212900	0.91122200
N	2.71922500	-1.89108600	0.04510200	C	5.07460500	-4.27311200	1.67597400
C	-2.91859900	-1.17417600	-1.09349000	H	5.16571000	-4.92367100	2.54065400
C	-4.89558800	-2.58480900	-0.52604700	C	3.90792200	-3.53551000	1.50367800
C	-6.06601600	-3.31903900	-0.35483400	H	3.09093300	-3.60134800	2.21228600
H	-6.87363200	-3.25461300	-1.07719900	C	3.80377900	-2.70224900	0.38715200
C	-6.17034800	-4.13958000	0.76492500	S	-0.02613400	-2.72492200	-0.01063100
H	-7.07351800	-4.72222700	0.91896600	B	1.41143800	-1.78130100	0.85975300
C	-5.12060300	-4.22263800	1.68646000	B	-1.44101600	-1.75456900	0.87328700
H	-5.21595700	-4.87299300	2.55082100	C	-1.08964900	2.56534000	1.66701400
C	-3.95023600	-3.49049400	1.51605600	C	-2.40105700	2.07771200	1.68677800
H	-3.13457200	-3.55956100	2.22582600	C	-0.66113300	3.42655800	2.67954700
C	-3.84098500	-2.65710600	0.40013600	C	-3.27190000	2.44770700	2.70830600
H	-1.59959900	-2.03267900	2.02950800	H	-2.73571200	1.40607100	0.90075100
H	-1.16620400	-0.43296800	1.04572800	C	-1.53330100	3.78761100	3.70785100
H	1.15720400	-0.45319400	1.03148100	H	0.35315200	3.81354600	2.67082300

C	-2.83796400	3.30040500	3.72392300	H	4.28636200	2.00759900	2.82871100
H	-4.28860000	2.06450300	2.71410000	H	5.16049500	4.12164900	1.85309100
H	-1.18841900	4.45150300	4.49598700	C	-0.51855600	3.20286300	-1.13169400
H	-3.51543700	3.58197100	4.52542300	C	-1.28835200	4.34126000	-0.87553700
C	1.69926300	2.74596300	0.74412600	C	-0.12644900	2.92107500	-2.44411000
C	2.18981400	3.93744400	0.20432500	C	-1.66238100	5.18489200	-1.92130700
C	2.46477300	2.05556800	1.68963500	H	-1.60093900	4.56843700	0.13899600
C	3.43422200	4.42796800	0.60143500	C	-0.49666000	3.76823200	-3.48634000
H	1.60392900	4.48171800	-0.52943900	H	0.46910300	2.03807100	-2.65417600
C	3.70169400	2.55235900	2.09253700	C	-1.26737200	4.90068600	-3.22708700
H	2.09259200	1.12577800	2.11017000	H	-2.26535600	6.06447800	-1.71244000
C	4.19126500	3.73862000	1.54563400	H	-0.18796000	3.53665300	-4.50181300
H	3.80958700	5.35142400	0.16888200	H	-1.56249700	5.55730400	-4.04098500

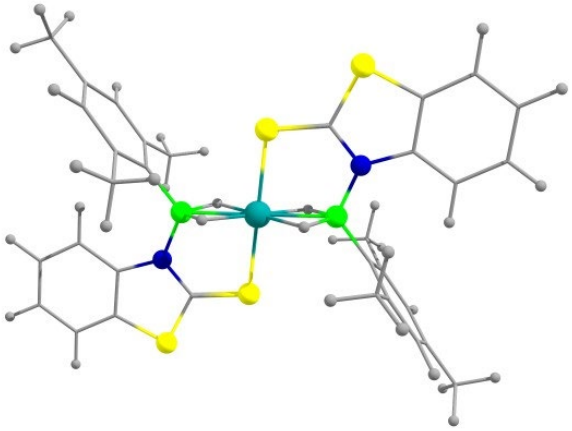

Figure S44. Optimized geometry of *trans*-**4**.

Cartesian coordinates for the calculated structure of *trans*-**4** (in Å).

Ru	-0.00000300	-0.00000100	-0.00001700	H	-2.02642800	1.48359600	-2.73431400
				C	-5.47262000	5.02266900	-0.00041900
B	-2.17141400	0.08603500	0.00001300	H	-6.54278400	4.77986800	-0.00015800
C	-3.08783000	1.38529200	-0.00007100	H	-5.27939100	5.63535300	-0.88610400
C	-3.48103900	1.99472900	-1.21457800	H	-5.27904300	5.63572500	0.88493100
C	-4.23980700	3.16810700	-1.19502700	C	-4.20484900	-1.65190900	0.00018000
H	-4.53282600	3.62108100	-2.14082900	C	-5.30909800	-0.79345400	0.00034800
C	-4.63044300	3.77415300	-0.00031500	H	-5.16976100	0.27873900	0.00039500
C	-4.23934600	3.16863900	1.19452100	C	-6.58757400	-1.34286900	0.00045800
H	-4.53200600	3.62204700	2.14022700	H	-7.44314700	-0.67419400	0.00058800
C	-3.48057600	1.99527100	1.21431800	C	-6.78999000	-2.72582700	0.00041100
C	-3.10309900	1.40232000	2.55014600	H	-7.79797200	-3.12934100	0.00050000
H	-3.61910000	1.91573600	3.36638800	C	-5.70117000	-3.59103400	0.00026400
H	-2.02538800	1.48482500	2.73373300	H	-5.84074700	-4.66750300	0.00024100
H	-3.35873500	0.33875900	2.61451600	C	-4.42182500	-3.04196600	0.00015500
C	-3.10406800	1.40116600	-2.55027600	C	-2.02384900	-2.39654800	-0.00000700
H	-3.62038300	1.91419900	-3.36656300	S	-0.34330600	-2.34017600	-0.00007300
H	-3.35972100	0.33757500	-2.61405400	S	-2.90146400	-3.90615300	0.00001100

N	-2.83766300	-1.30874500	0.00005400
H	-1.34543500	0.10925800	-1.07724400
H	-1.34544300	0.10924500	1.07721900
B	2.17140800	-0.08603800	0.00002600
C	3.08782400	-1.38529600	-0.00006300
C	3.48051100	-1.99533800	1.21430600
C	4.23930900	-3.16869500	1.19448400
H	4.53192700	-3.62214200	2.14018400
C	4.63046500	-3.77413900	-0.00036000
C	4.23987200	-3.16803300	-1.19506400
H	4.53293900	-3.62096400	-2.14087200
C	3.48110300	-1.99466300	-1.21459000
C	3.10421000	-1.40100500	-2.55026600
H	3.62048800	-1.91404800	-3.36656700
H	2.02656600	-1.48330900	-2.73433100
H	3.35997700	-0.33743600	-2.61397900
C	3.10295500	-1.40248400	2.55015700
H	3.61888300	-1.91598600	3.36639400
H	3.35861800	-0.33893600	2.61464200
H	2.02523000	-1.48497500	2.73365700
C	5.47265600	-5.02264600	-0.00051600
H	6.54281800	-4.77983400	-0.00037300
H	5.27917600	-5.63568700	0.88486500
H	5.27934200	-5.63534900	-0.88617000
C	4.20484300	1.65190500	0.00024800
C	5.30909300	0.79345000	0.00047700
H	5.16975700	-0.27874300	0.00057000
C	6.58756800	1.34286500	0.00058500
H	7.44314200	0.67419000	0.00076000
C	6.78998500	2.72582300	0.00048000
H	7.79796700	3.12933800	0.00056400
C	5.70116500	3.59103000	0.00028000
H	5.84074100	4.66750000	0.00021500
C	4.42182000	3.04196200	0.00017300
C	2.02384400	2.39654500	0.00002000
S	0.34330100	2.34017300	-0.00007100
S	2.90145900	3.90614900	-0.00002200
N	2.83765800	1.30874100	0.00011700
H	1.34540300	-0.10930000	1.07723900
H	1.34546200	-0.10920900	-1.07722300

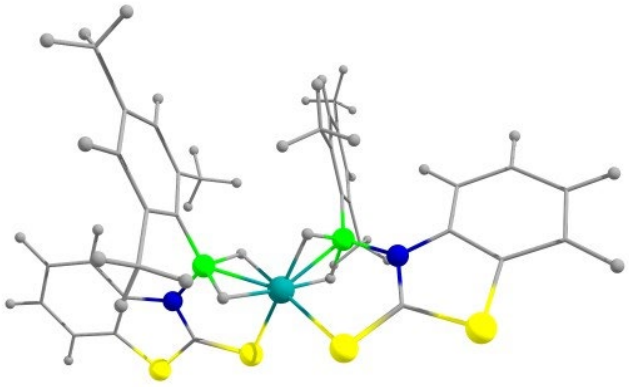

Figure S45. Optimized geometry of *cis*-**4**.

Cartesian coordinates for the calculated structure of *cis*-**4** (in Å).

Ru	-0.00008400	-1.22653400	-0.00039500
C	-4.44839400	-0.59716200	-0.44272600
C	-5.23394300	-1.52320400	-1.15354700
C	-6.60583700	-1.35442100	-1.32039000
C	-7.20422400	-0.23090300	-0.76037900
C	-6.43469200	0.69545100	-0.05051500
C	-5.06372200	0.52753500	0.11661000
N	-3.08701200	-0.95509200	-0.39549900
C	-2.82952100	-2.11927800	-1.03726900
S	-4.24950400	-2.84012400	-1.75077800
S	-1.30233500	-2.82095400	-1.14772600
B	-1.88427600	-0.22629100	0.26370800
H	-1.32818400	-1.16325500	1.09636400
H	-0.99915800	-0.00739300	-0.74594800
C	4.44825800	-0.59757500	0.44303100
C	5.23349500	-1.52371100	1.15407700
C	6.60536000	-1.35506000	1.32132800
C	7.20402800	-0.23159800	0.76150800
C	6.43479600	0.69485100	0.05143100
C	5.06385800	0.52707200	-0.11609700

N	3.08683400	-0.95536500	0.39541300
C	2.82906300	-2.11953300	1.03707900
S	4.24876200	-2.84054800	1.75098400
S	1.30177800	-2.82109500	1.14709100
B	1.88435900	-0.22645800	-0.26420700
H	0.99893500	-0.00750900	0.74524800
H	1.32853200	-1.16311900	-1.09696900
H	-7.18984600	-2.08333500	-1.87338700
H	-8.27269100	-0.07671800	-0.87645500
H	-6.91083600	1.56916600	0.38418700
H	-4.48200700	1.25177400	0.67005600
H	7.18913300	-2.08404500	1.87448300
H	8.27247700	-0.07752500	0.87789500
H	6.91115800	1.56852600	-0.38311400
H	4.48237200	1.25138500	-0.66969300
C	-2.15443500	1.11149200	1.07935700
C	-2.41302500	1.07672400	2.46993100
C	-2.10805400	2.37196500	0.43692200
C	-2.60888000	2.26779900	3.17515700
C	-2.31132500	3.54128400	1.17533300
C	-2.55660100	3.51355500	2.54912900
H	-2.81515900	2.21934700	4.24316700
H	-2.28187000	4.50013200	0.66006800
C	-2.50381300	-0.22741700	3.22493200
H	-3.19606000	-0.93027300	2.74830600
H	-1.53014400	-0.72754600	3.28203200
H	-2.85339700	-0.06307400	4.24813300
C	-1.86627800	2.48841100	-1.04845900
H	-2.54998300	1.85505200	-1.62482500
H	-2.00691900	3.51880300	-1.38698900
H	-0.84624900	2.18927700	-1.31444300
C	-2.74094300	4.78647500	3.33220400
H	-3.20481400	5.56898500	2.72371300
H	-3.36672500	4.62700300	4.21555200
H	-1.77737800	5.17698600	3.68281300
C	2.15486400	1.11144700	-1.07954800
C	2.41357100	1.07684800	-2.47009100
C	2.10849000	2.37183300	-0.43694400
C	2.60954900	2.26800700	-3.17515300
C	2.31187200	3.54123600	-1.17517700
C	2.55726300	3.51367600	-2.54896400
H	2.81595600	2.21966900	-4.24314400
H	2.28242900	4.50002600	-0.65980500
C	1.86651800	2.48805500	1.04842000
H	2.54962800	1.85404200	1.62476100
H	2.00784000	3.51825500	1.38725900
H	0.84620900	2.18959800	1.31410700
C	2.50428700	-0.22719800	-3.22526900
H	3.19582800	-0.93050000	-2.74829500
H	1.53040100	-0.72682700	-3.28315700
H	2.85467700	-0.06282200	-4.24819000
C	2.74171800	4.78670100	-3.33184700
H	3.20517200	5.56922900	-2.72306700
H	3.36792600	4.62742500	-4.21493200
H	1.77824500	5.17707500	-3.68286600

III References

1 M. Zafar, R. Ramalakshmi, K. Pathak, A. Ahmad, T. Roisnel, S. Ghosh, *Chem. Eur. J.,* 2019, **25**, 13537-13546.

2 K. Smith, A. Pelter, Z. Jin, *Angew. Chem., Int. Ed. Engl.,* 1994, **33**, 851-853.

3 G. E. Ryschlewitsch, K. C. Nainan, S. R. Miller, L. J. Todd, W. J. Dewkett, M. Grace, H. Beall, M. F. Hawthorne, R. Leyden, *Inorg. Synth.,* 2007, **15**, 111-118.

4 (a) J. J. Led, H. Gesmar, *Chem. Rev.,* 1991, **91**, 1413–1426; (b) L. Yang, R. Simionescua, A. Lough, H. Yan, *Dyes and Pigments*, 2011, **91**, 264-267.

5 (a) G. M. Sheldrick, *Acta Cryst.,* 2015, **A71**, 3–8. (b) G. M. Sheldrick, SHELXS97 and SHELXL97, University of Gottingen: Germany, 1997.

6 G. M. Sheldrick,. *Acta Cryst.,* 2015, **C71**, 3–8.

7 O. V. Dolomanov, L. J. Bourhis, R. J. Gildea, J. A. K. Howard, H. Puschmann, *J. Appl. Crystallogr.,* 2009, **42**, 339-341.

8 A. D. Becke, A. D. *J. Chem. Phys.,* 1993, **98**, 5648-5652. (b) Perdew, J. P.; Wang, Y. *Physical Review B,* 1992, **45**, 13244-13249.

9 Gaussian 09, Revision C.01, M. J. Frisch, G. W. Trucks, H. B. Schlegel, G. E. Scuseria, M. A. Robb, J. R. Cheeseman, G. Scalmani, V. Barone, B. Mennucci, G. A. Petersson, H. Nakatsuji, M. Caricato, X. Li, H. P. Hratchian, A. F. Izmaylov, J. Bloino, G. Zheng, J. L. Sonnenberg, M. Hada, M. Ehara, K. Toyota, R. Fukuda, J. Hasegawa, M. Ishida, T. Nakajima, Y. Honda, O. Kitao, H. Nakai, T. Vreven, J. A. Montgomery, Jr., J. E. Peralta, F. Ogliaro, M. Bearpark, J. J. Heyd, E. Brothers, K. N. Kudin, V. N. Staroverov, T. Keith, R. Kobayashi, J. Normand, K. Raghavachari, A. Rendell, J. C. Burant, S. S. Iyengar, J. Tomasi, M. Cossi, N. Rega, J. M. Millam, M. Klene, J. E. Knox, J. B. Cross, V. Bakken, C. Adamo, J. Jaramillo, R. Gomperts, R. E. Stratmann, O. Yazyev, A. J. Austin, R. Cammi, C. Pomelli, J. W. Ochterski, R. L. Martin, K. Morokuma, V. G. Zakrzewski, G. A. Voth, P. Salvador, J. J. Dannenberg, S. Dapprich, A. D. Daniels, O. Farkas, J. B. Foresman, J. V. Ortiz, J. Cioslowski, D. J. Fox, Gaussian, Inc., Wallingford CT, 2010.

10 (a) D. Andrae, U. Häußermann, M. Dolg, H. Stoll, H. Preuß, *Theor. Chim. Acta*, 1990, **77**, 123-141. (b) A. Bergner, M. Dolg, W. chle, H. Stoll, Preu; Heinzwerner *Mol. Phys.,* 1993, **80**, 1431-1441.

11 P. C. Hariharan, J. A. Pople, *Theor. Chim. Acta* 1973, **28**, 213-222.

12 (a) F. J. London, *J. Phys. Radium* 1937, **8**, 397-409, (b) R. Ditchfield, *Mol. Phys.* 1974, **27**, 789-807, (c) K. Wolinski, J. F.Hinton, P. Pulay, *J. Am. Chem. Soc.,* 1990, **112**, 8251-8260.

13 T. P. Onak, H. L. Landesman, R. E. Williams, I. Shapiro, *J. Phys.Chem.,* 1959, **63**, 1533-1535.

14 NBO Program 6.0, E. D. Glendening, J. K. A. E. Badenhoop, Reed, J. E. Carpenter, J. A. Bohmann, C. M. Morales, C. R. Landis, F. Weinhold, Theoretical Chemistry Institute, University of Wisconsin, Madison, WI, 2013.

15 K. Wiberg, *Tetrahedron,* 1968, 24, 1083-1096.

16 T. Lu, F. Chen, Multiwfn: A multifunctional wavefunction analyzer. *J. Comput. Chem.* 2012, **33**, 580-592.

17 Chemcraft - graphical software for visualization of quantum chemistry computations https://www.chemcraftprog.com.